



Isotopically Light Cd in Sediments Underlying Oxygen Deficient Zones

Lena Chen^{1,3*}, Susan H. Little^{2,3}, Katharina Kreissig³, Silke Severmann⁴ and James McManus⁵

¹School of Earth and Environment, University of Leeds, Leeds, United Kingdom, ²Department of Earth Sciences, University College London, London, United Kingdom, ³Department of Earth Science and Engineering, Imperial College London, London, United Kingdom, ⁴Department of Marine and Coastal Science, Rutgers University, New Brunswick, NJ, United States, ⁵Bigelow Laboratory for Ocean Sciences, East Boothbay, ME, United States

OPEN ACCESS

Edited by:

Martyn Tranter,
Aarhus University, Denmark

Reviewed by:

Ruifang Xie,
GEOMAR Helmholtz Center for Ocean
Research Kiel, Germany
Claudia Ehrlert,
University of Oldenburg, Germany

*Correspondence:

Lena Chen
eelch@leeds.ac.uk

Specialty section:

This article was submitted to
Geochemistry,
a section of the journal
Frontiers in Earth Science

Received: 30 October 2020

Accepted: 04 February 2021

Published: 18 March 2021

Citation:

Chen L, Little SH, Kreissig K, Severmann S and McManus J (2021) Isotopically Light Cd in Sediments Underlying Oxygen Deficient Zones. *Front. Earth Sci.* 9:623720. doi: 10.3389/feart.2021.623720

Cadmium is a trace metal of interest in the ocean partly because its concentration mimics that of phosphate. However, deviations from the global mean dissolved Cd/PO₄ relationship are present in oxygen deficient zones, where Cd is depleted relative to phosphate. This decoupling has been suggested to result from cadmium sulphide (CdS) precipitation in reducing microenvironments within sinking organic matter. We present Cd concentrations and Cd isotope compositions in organic-rich sediments deposited at several upwelling sites along the northeast Pacific continental margin. These sediments all have enriched Cd concentrations relative to crustal material. We calculate a net accumulation rate of Cd in margin settings of between 2.6 to 12.0 × 10⁷ mol/yr, higher than previous estimates, but at the low end of a recently published estimate for the magnitude of the marine sink due to water column CdS precipitation. Cadmium in organic-rich sediments is isotopically light ($\delta^{114/110}\text{Cd}_{\text{NIST-3108}} = +0.02 \pm 0.14\text{\textperthousand}$, $n = 26$; 2 SD) compared to deep seawater ($+0.3 \pm 0.1\text{\textperthousand}$). However, isotope fractionation during diagenesis in continental margin settings appears to be small. Therefore, the light Cd isotope composition of organic-rich sediments is likely to reflect an isotopically light source of Cd. Non-quantitative biological uptake of light Cd by phytoplankton is one possible means of supplying light Cd to the sediment, which would imply that Cd isotopes could be used as a tracer of past ocean productivity. However, water column CdS precipitation is also predicted to preferentially sequester light Cd isotopes from the water column, which could obfuscate Cd as a tracer. We also observe notably light Cd isotope compositions associated with elevated solid phase Fe concentrations, suggesting that scavenging of Cd by Fe oxide phases may contribute to the light Cd isotope composition of sediments. These multiple possible sources of isotopically light Cd to sediments, along with evidence for complex particle cycling of Cd in the water column, bring into question the straightforward application of Cd isotopes as a paleoproductivity proxy.

Keywords: CdS precipitation, oxygen deficient zones, continental margin, isotope fractionation, cadmium

INTRODUCTION

Dissolved cadmium (Cd) displays typical nutrient-type behavior in the oceans (e.g., Bruland et al., 2014), despite its known toxicity (e.g., Brand et al., 1986; Waldron and Robinson, 2009). The reason for its nutrient-type behavior is not fully understood; to date, only one biological function of Cd has been identified, in which it replaces Zn in the enzyme carbonic anhydrase (Price and Morel, 1990; Lane et al., 2005; Xu et al., 2008). Nevertheless, dissolved Cd has a spatial distribution akin to the macronutrient phosphate (PO_4) (e.g., Boyle et al., 1976; Bruland, 1980), and Cd/Ca ratios in calcareous microfossils have been utilized as a proxy for past oceanic P distributions (e.g., Marchitto and Broecker, 2006).

Cadmium isotopes in marine carbonates and organic-rich sediments are emerging as a potential tracer of past ocean productivity (Georgiev et al., 2015; John et al., 2017; Hohl et al., 2017, 2019), contingent on the observation that biological uptake of Cd in the surface ocean is associated with preferential uptake of the light isotope (e.g., Lacan et al., 2006; Ripperger et al., 2007). However, deviations from the global ocean Cd/PO₄ relationship are observed in oxygen deficient zones (ODZ) of the modern ocean (e.g., van Geen et al., 1995; Janssen et al., 2014; Middag et al., 2018), deviations that are in some cases associated with Cd isotope fractionation (e.g., Conway and John 2015a). Thus, further work is required to constrain the cycling of Cd and its isotopes in the ocean.

Stable isotopes are a useful tool to constrain the whole oceanic mass balance of an element. The Cd isotope composition of seawater, denoted here as $\delta^{114/110}\text{Cd}_{\text{NIST SRM 3108}}$ (Eqn. 1), ranges from 0 to +5‰ at the surface, with a uniform deep water average of about +0.3‰ (Ripperger et al., 2007; Xue et al., 2013; Conway and John, 2015a, 2015b; Xie et al., 2017, 2019a, 2019b; John et al., 2018; Sieber et al., 2019a, 2019b; George et al., 2019; Guinoiseau et al., 2019). The isotopic composition of Cd inputs to the ocean are not well constrained, but two studies find aerosol-borne Cd and dissolved riverine Cd to have an isotopic composition similar to lithogenic material at 0.0‰ and $+0.2 \pm 0.1\text{‰}$ respectively (Lambelet et al., 2013; Bridgestock et al., 2017). The deep oceans are isotopically heavier than lithogenic Cd; therefore, mass balance requires an isotopically light sink for Cd in sediments.

To date only Fe-Mn crusts—the chemical signatures of which are often used as a proxy for removal to Fe-Mn oxide phases in oxygenated deep-sea settings—have been analysed for their $\delta^{114}\text{Cd}$ values. Fe-Mn crusts have Cd isotope compositions similar to the deep ocean $\delta^{114}\text{Cd}$ value, at about +0.3‰ (Schmitt et al., 2009; Horner et al., 2010), and therefore cannot be the isotopically light output flux required to balance the Cd budget.

Organic-rich sedimentary settings along productive continental margins are considered a second important sink for Cd (e.g., van Geen et al., 1995; Morford and Emerson, 1999; Little et al., 2015). Organic matter derived from biological primary productivity in the upper water column is one important source of Cd to margin sediments (Elderfield et al., 1981; Rosenthal et al., 1995). In culture, biological uptake is associated with a preference for isotopically light Cd, consistent

with the observed isotopically heavy residual dissolved pool in surface seawater (e.g., Ripperger et al., 2007). Organic matter is thus one isotopically light source of Cd to margin sediments (e.g., Yang et al., 2015, 2018; John et al., 2018; Janssen et al., 2019). A second possible source is the precipitation of CdS, either in reducing microenvironments within sinking organic material (e.g., Janssen et al., 2014; Bianchi et al., 2018; Guinoiseau et al., 2019), or in bottom waters proximal to an anoxic sediment-water interface (Xie et al., 2019b; Plass et al., 2020). Consistent with an isotopically light particulate source of Cd to sediments, Janssen et al. (2019) observed isotopically light particles (size range: 0.8–51 μm), ranging from -0.5 to -0.2‰ , at water depths of 200–800 m in the northeast Pacific. They propose that the export and burial of these light particulate phases in organic-rich shelf sediments may balance the oceanic Cd budget (Janssen et al., 2019).

As yet, no Cd isotope compositions from modern organic-rich sediments have been reported. Here, we present data for sediments from the northeast Pacific margin. Our dataset supports the suggestion of an isotopically light sink for Cd in margin settings, and places improved constraints on the Cd mass balance and Cd isotope budget of the oceans. Finally, we consider the implications of our data for the utility of Cd isotopes as a tracer of past ocean productivity.

MATERIALS AND METHODS

Sites and Sampling

Samples were selected from the northeast Pacific margin (Table 1; Figure 1), specifically, from four of the California Borderland Basins (Santa Barbara, Santa Monica, San Nicolas and Tanner Basin), and three sites along the Mexican margin (Pescadero slope, Soledad Basin and Magdalena margin). Sediment cores were collected using a multicorer, as described by McManus et al. (2006). The sites are situated in regions of elevated productivity resulting from coastal upwelling, with water column oxygen depletion at intermediate depth as a consequence of organic matter remineralization. The seven sites span a range of water column oxygen conditions and resultant sedimentary diagenetic regimes (Table 1). They also vary in depositional setting, from restricted basins to open continental margin. The sites and samples have been extensively described previously (see: McManus et al., 2006; Poulson-Brucker et al., 2009; Chong et al., 2012; Little et al., 2016; Little et al., 2017) and are thus only briefly introduced here.

California Borderland Basins

The southern California Borderland Basins are separated from one another by their silled topography, thus they exhibit lower oxygen concentrations at intermediate depth and in bottom waters compared to equivalent depths along the open margin (Emery, 1960). The enhanced upwelling generates an ODZ between the depths of 200 and 1,000 m. The basins are situated at a range of water depths and distances offshore, resulting in a range of low oxygen conditions in the region (Table 1).

TABLE 1 | Site descriptions, after Little et al. (2016).

Site	Lat °N	Long °W	Coring Depth (m)	Sill depth (m)	Basin depth (m)	Bottom water O ₂ (µM)	Diagenetic regime ^a	Sediment accumulation rate (mg/cm ² /y)	Organic C burial flux (mg/cm ² /y)	References
Santa Barbara Basin	34.3	120.0	493	475	600	0–10	Ferr	92	–	1
Santa Monica Basin	33.7	118.8	905	740	910	2–10	Ferr	16	0.7 ± 0.2	2
San Nicolas Basin	32.8	118.8	1750	1,100	1832	15–35	Mn–ferr	14	–	1
Tanner Basin	33.0	119.7	1,514	1,160	1,550	~30	Mn–ferr	12	0.8 ± 0.1	2
Soledad Basin	25.2	112.7	544	250	545	0	Ferr–sulf	50–90	3.7 ± 0.1	3,4,5
Pescadero slope	24.3	108.2	616	Na	Na	0.4	Ferr	77	–	3
Magdalena margin	23.5	111.6	692	Na	Na	0.9	Ferr–sulf	4–12	–	3

^aFerr—Ferruginous; Mn—Manganese rich; Sulf—Sulphidic.

Na—Not applicable.

References: 1. Poulson Brucker et al. (2009); 2. McManus et al. (2006); 3. Chong et al. (2012); 4. Silverberg et al. (2004); 5. Bralower and Thierstein (1987).

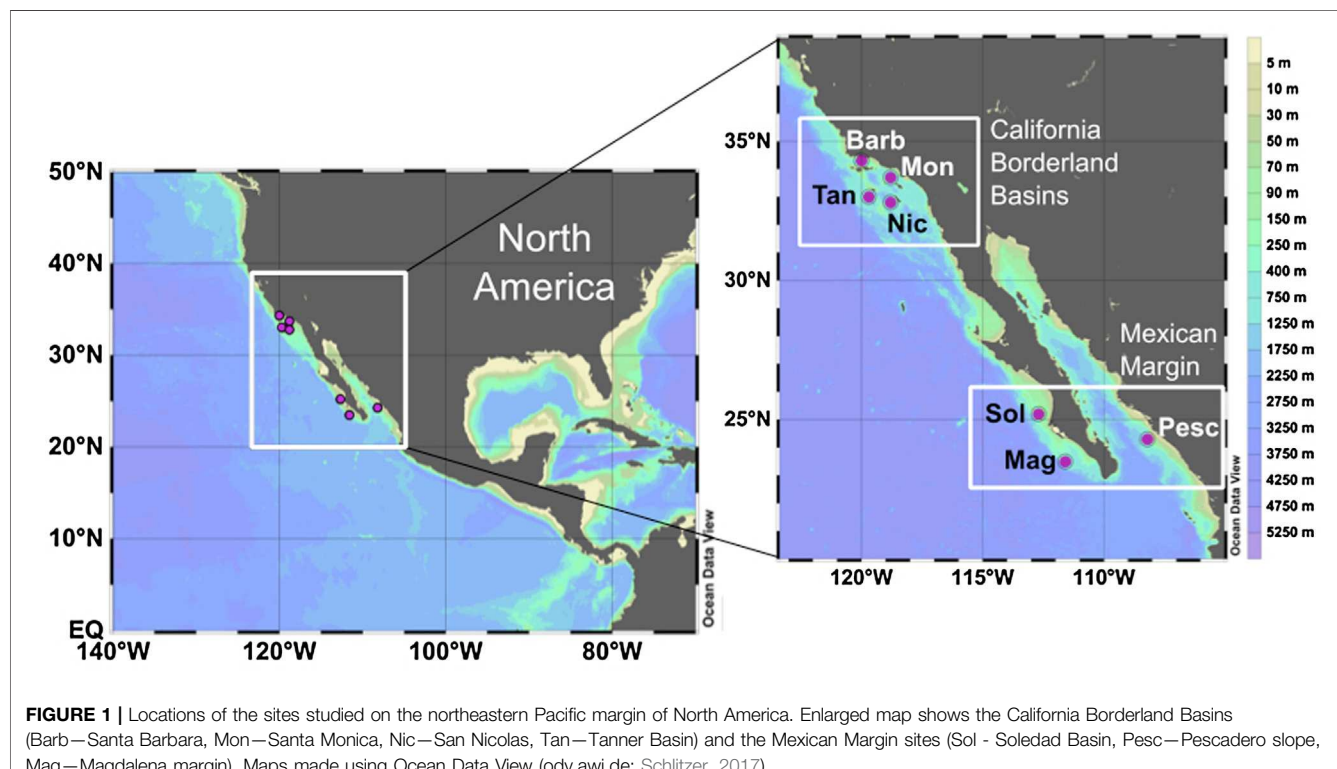


FIGURE 1 | Locations of the sites studied on the northeastern Pacific margin of North America. Enlarged map shows the California Borderland Basins (Barb—Santa Barbara, Mon—Santa Monica, Nic—San Nicolas, Tan—Tanner Basin) and the Mexican Margin sites (Sol - Soledad Basin, Pesc—Pescadero slope, Mag—Magdalena margin). Maps made using Ocean Data View (odv.awi.de; Schlitzer, 2017).

Santa Barbara and Santa Monica are nearshore basins. They are both within the Californian ODZ, thus display low bottom oxygen water conditions of <10 µM, with the Santa Barbara Basin being the most reducing. Both core sites have ferruginous shallow porewaters, which indicate that iron and sulphate reduction are likely to be the dominant electron transfer pathways (McManus et al., 1997; 1998). Santa Barbara has a high sediment accumulation rate (~90 mg/cm²/yr) compared to the other Borderland Basins (10–20 mg/cm²/yr), which can be attributed to a higher lithogenic input due to its location close to the continent (Thunell et al., 1995).

By comparison, the offshore basins, San Nicolas and Tanner, provide examples of lower carbon fluxes and higher oxygen concentrations. The San Nicolas and Tanner basins have sill

depths below the depth of the ODZ. They have higher bottom water oxygen contents than the nearshore basins, of between 15 and 35 µM, and are diagenetically similar, displaying Mn–Fe rich porewaters, although the Tanner Basin displays lower Fe and Mn than San Nicolas (Shaw et al., 1990; McManus et al., 1997; 1998). At these sites, organic matter is oxidized through a combination of terminal electron acceptors including oxygen, nitrate, Mn, Fe and sulphate.

Mexican Margin

Along the Mexican margin, the sites examined (Pescadero slope, Soledad Basin and Magdalena margin) have considerably lower bottom water oxygen concentrations

($<1\text{ }\mu\text{M}$) than the Californian Borderland Basins. The ODZ extends more than 1,500 km off the coast of Mexico at depths of 500–1,000 m. The sediment coring depths in this study are all within the ODZ. Therefore, there is likely to be limited bioturbation and excellent preservation of laminated sediments in the cores.

The Pescadero slope is an open margin site on the eastern edge of the mouth of the Gulf of California (Figure 1) and receives extensive continental input from the Sierra Madre Occidental Mountains (e.g., Berelson et al., 2005; Chong et al., 2012). The core was collected at a depth of 616 m within the ODZ. The porewaters have high concentrations of dissolved Fe, rapidly increasing from 3 μM at the surface and to a maximum of $\sim 400\text{ }\mu\text{M}$ at a depth of 8 cm (Chong et al., 2012).

Soledad Basin and the Magdalena margin are on the western open ocean margin side of Baja California (Figure 1). The core in the Soledad Basin was collected at a water depth of 544 m, close to the deepest point of the basin. This basin is isolated from the open ocean by a sill at approximately 250 m depth (Silverberg et al., 2004). A prior report noted that the sediments are laminated with coccolith laminae (van Geen et al., 2003). By contrast, the Magdalena margin site represents an open, unrestricted continental margin setting. It has a core depth of 692 m and the upper 1–2 cm of sediment is bioturbated. Both locations have dissolved sulphide in the porewaters, increasing from ~ 10 and 2 μM at the surface to >40 and $>20\text{ }\mu\text{M}$ below 8 and 20 cm depth in the Soledad Basin and Magdalena margin respectively (Chong et al., 2012). Unlike the Pescadero slope, these two locations receive very little lithogenic input. Nevertheless, Soledad Basin also has a high sediment accumulation rate of $50\text{--}90\text{ mg/cm}^2/\text{yr}$ (Silverberg et al., 2004). This high sediment accumulation rate at Soledad Basin indicates elevated productivity, which is supported by a high organic carbon burial flux of $3.7\text{ mg/cm}^2/\text{yr}$ at this site (Bralower and Thierstein, 1987).

Analytical Methods

Porewater Analyses

Porewater samples were collected and sampled from sediments as described in prior publications (McManus et al., 1997, 1998, 2006; Severmann et al., 2006; Chong et al., 2012) and porewater Fe and Mn were reported previously for most of the sites discussed here (see references in Table 1). However, Santa Barbara and San Nicholas porewater results were not published previously. For these sites porewater Fe and Mn were prepared for analysis by a 20-fold dilution and standard additions of a surface sample from each core. Samples were measured on an Agilent 7500ce quadrupole inductively coupled plasma mass spectrometer (ICP-MS) equipped with a collision cell (using hydrogen gas) at the University of California, Riverside. Analytical precision was $\sim 7\%$ (2 standard deviation) for both Fe and Mn.

Sample Preparation for Cd Isotope Analysis

All sample preparation was conducted in laminar flow hoods (ISO-4). Sediment samples were digested at ETH Zürich (Little et al., 2016). All further sample preparation work

for the Cd isotope analysis was conducted in the MAGIC clean room laboratories at Imperial College London. Concentrated HCl, HNO_3 and HF were purified in Teflon DST-1000 Acid Purification Systems from Savillex and diluted to the required concentration with MilliQ water (18.2 $\text{M}\Omega$) from a Milli-Q Advantage dispensing system. $\sim 500\text{ mg}$ of each sample were digested, as previously described by Little et al. (2016). In summary, each sample powder was pre-digested with dilute nitric acid at room temperature to dissolve carbonate. The sample and supernatant were then dried down, before complete digestion on a hotplate with a 3:1 mix of concentrated HF and HNO_3 . Once digested and dried, samples were treated with concentrated HNO_3 three times to redissolve fluoride salts, before final dissolution in 25 ml 7M HCl. Elemental analysis on an aliquot of these solutions was conducted at ETH Zürich on a Thermo Scientific ELEMENT XR ICP-MS (Little et al., 2016).

An aliquot containing $\sim 100\text{ ng}$ of Cd was then sub-sampled at Imperial College London and spiked with a ^{111}Cd – ^{113}Cd double spike to obtain a spike to sample-derived (S/N) Cd ratio of ~ 1 (Xue et al., 2012). In addition to the samples, two procedural blanks, a column blank, and three aliquots of a USGS basalt reference material (BCR-2) were prepared for Cd isotope analysis. Procedural blanks were $\sim 46\text{ pg}$ Cd, up to a maximum of 0.6% of the Cd content in the smallest sample.

A three-stage column chemistry procedure following Ripperger and Rehkämper (2007) and Xue et al. (2012) was used to separate Cd from the matrix. Briefly, anion-exchange chromatography was performed for the first two stages using AG1-X8 anion-exchange resin. The first two stages differ in column size (2 ml quartz glass columns and 150 μL shrink fit Teflon columns) and resin grain size (100–200 and 200–400 mesh). The last stage of the separation chemistry utilized the same small Teflon columns as during the second-stage procedure, but Biorad Eichrom TRU resin was used to separate Sn and traces of Nb, Zr, Mo in the sample.

Finally, liquid-liquid extraction with *n*-heptane was employed to remove any organic compounds that could be released from the resin (Murphy et al., 2016). The *n*-heptane was pre-cleaned through liquid–liquid extraction with 6M HCl, following the detailed procedure outlined in Murphy et al. (2016). Afterward, the samples were dried twice and re-dissolved with a few drops of concentrated HNO_3 and taken up in 1 ml 2% HNO_3 for mass spectrometry.

Cadmium Isotope Compositions

Cadmium isotope ratio analyses were conducted on the Nu Plasma high resolution multi collector ICP-MS (HR MC-ICP-MS) equipped with a DSN-100 desolvation system and a MicroMist glass nebulizer, with an uptake rate of $\sim 120\text{ }\mu\text{L}/\text{min}$. The ion masses of 114 (Cd), 113 (Cd), 112 (Cd), 111 (Cd) along with 117 (Sn) and 115 (In) were measured simultaneously in low-resolution mode with Faraday cups. The instrumental sensitivity for Cd ranged from 240–310 V/ ppm. The S/N ratio and total Cd concentration of the samples matched those of simultaneously measured spiked standard reference

TABLE 2 | Summary of results, including bulk sediment Cd isotope compositions and Cd, Al and Fe concentrations.

Location	Site	Sample	Depth in sediment (cm)	Coring Depth (m)	Cd (µg/g)	Al (wt%)	Fe (wt%)	Org C* (wt%)	$\delta^{114}\text{Cd}$ (‰)	2σ or 2SD	n ^a
California margin	Santa Barbara Basin	MC17_1	1–1.5	493	0.92	6.6	3.3	3.01	-0.02	0.07	2
		MC17_8	8–8.5		0.8	6.0	3.2	1.50	-0.03	0.06	2
		MC17_40	32–34		0.92	6.3	3.3	2.93	0.04	0.03	2
	Santa Monica Basin	8B3	1–2	905	2.88	5.4	3.2	5.73	0.08	0.05	3
		8B5	3–4		0.81	6.2	4.0	5.23	-0.08	0.03	2
		8B8	6–9		0.98	6.2	3.9	4.19	-0.19	0.05	1
		8B15	18–22		0.99	6.1	3.9	4.50	-0.06	0.04	2
	San Nicolas Basin	MC37 2.5–3	2.5–3	1,750	0.53	4.8	2.7	4.92	-0.04	0.05	1
		MC37 4–4.5	4–4.5		0.65	5.1	2.7	4.85	0.03	0.05	1
		MC37 14–15	14–15		0.65	4.7	2.1	4.25	0.09	0.05	1
		MC37 32–34	32–34		0.92	5.1	3.0	4.41	0.00	0.05	1
	Tanner Basin	12B3	1–2	1,514	1	3.3	1.7	6.69	0.08	0.04	1
		12B5	3–4		0.96	3.3	1.8	6.35	0.11	0.05	1
		12B7	6–9		0.76	3.0	1.5	5.96	0.03	0.04	1
		12B12	12–15		0.67	3.7	1.7	4.31	0.02	0.05	1
Mexican margin	Pescadero slope	Pesc_2	2–3	616	0.69	6.0	2.3	3.55	-0.02	0.05	1
		Pesc_11	11–12		0.70	6.5	2.4	3.45	-0.02	0.06	1
		Pesc_22	22–24		0.74	6.8	2.6	3.07	0.04	0.06	2
		Pesc_30	30–32		0.77	6.4	2.4	3.62	-0.08	0.04	1
	Soledad Basin	Sol2_1	1–2	544	1.88	3.8	1.9	6.47	0.06	0.08	2
		Sol2_11	11–12		1.90	4.1	2.0	6.39	0.04	0.06	1
		Sol2_20	20–22		2.38	3.8	2.0	6.66	0.09	0.02	2
		Sol2_30	30–32		2.15	4.2	2.0	6.23	0.10	0.06	1
	Magdalena margin	MagD_0	0–1	692	1.48	2.3	1.3	10.03	0.09	0.05	1
		MagD_4	4–5		2.75	2.3	1.1	11.71	0.08	0.05	1
		MagD_6	6–7		2.91	2.2	1.0	12.68	0.04	0.05	2

^aNumber of replicates run through separation chemistry or mass spectrometric analysis, $\delta^{114}\text{Cd}$ values are presented as means and uncertainties are the 2SD of those values.

*Organic Carbon data from Little et al. (2016).

solutions NIST SRM 3108 (NIST) and BAM I012 (BAM) to within $\pm 10\%$.

Instrumental mass bias was corrected using the double-spike technique described by Xue et al. (2012). Data reduction was carried out offline utilizing the iterative approach of Siebert et al. (2001). The Cd isotope ratios were then reported relative to the bracketing NIST Cd standards in delta notation:

$$\delta^{114/110}\text{Cd} = \delta^{114}\text{Cd} = \left[\frac{(^{114}\text{Cd}/^{110}\text{Cd})_{\text{Sample}}}{(^{114}\text{Cd}/^{110}\text{Cd})_{\text{NIST SRM 3108}}} - 1 \right] \times 1000 \quad (1)$$

Uncertainties reported in **Table 2** are either internal 2σ errors, which represent the within-run uncertainty on each individual Cd isotope analysis, or for duplicate analyses uncertainties are the 2SD of those values. The long-term external reproducibility is calculated based on multiple measurements of the secondary standard BAM ($-1.37 \pm 0.05\%$ 2SD, $n = 12$) and the BCR-2 reference material ($0.02 \pm 0.03\%$, $n = 3$).

RESULTS

Sediment Core Data

Cadmium concentrations presented here are normalized to Al in order to account for the presence of Cd from detrital silicates (**Figure 2**). All samples from all sites display elevated Cd/Al ratios

compared to the upper continental crust ($\text{Cd/Al}_{\text{UCC}} = 0.011 \times 10^{-4}$, Rudnick and Gao, 2003; **Figure 2**), indicating significant bioauthigenic enrichment (see also **section 4.1**). We define 'bioauthigenic' Cd here to include both chemically precipitated and biological Cd sources (i.e., non-lithogenic Cd). Sediment Cd/Al ratios range from 0.1 to 1.3×10^{-4} . The Magdalena margin and Soledad Basin sediment cores are distinctly more enriched in Cd than the cores from the other sites with the average downcore Cd/Al of 1.05×10^{-4} and 0.52×10^{-4} respectively. The Cd/Al ratio of the surface-most sample from Santa Monica is also notably elevated (0.53×10^{-4}) compared to samples deeper in the sediment core (at $\sim 0.15 \times 10^{-4}$) and other California Borderland Basin sites ($\leq 0.3 \times 10^{-4}$). This surface anomaly could reflect a recent anthropogenic source of metals, as previously reported for this site (Finney and Huh, 1989; Bruland et al., 1994).

Sediment Cd isotope compositions range from -0.19 to $+0.11\text{‰}$, with limited $\delta^{114}\text{Cd}$ variability between sites (**Table 2**; **Figure 2**). This range of values is isotopically lighter than global deep seawater, which has an average $\delta^{114}\text{Cd}$ value of about $+0.3\text{‰}$ (Ripperger et al., 2007; Xue et al., 2013; Abouchami et al., 2014; Conway and John, 2015a, 2015b; Xie et al., 2017, 2019a, 2019b; John et al., 2018; Sieber et al., 2019a, 2019b; George et al., 2019; Guinoiseau et al., 2019). The most reducing site of the California Borderland Basins, Santa Barbara, has an average $\delta^{114}\text{Cd}$ of $0.00 \pm 0.04\text{‰}$ (errors reported here are 1 standard

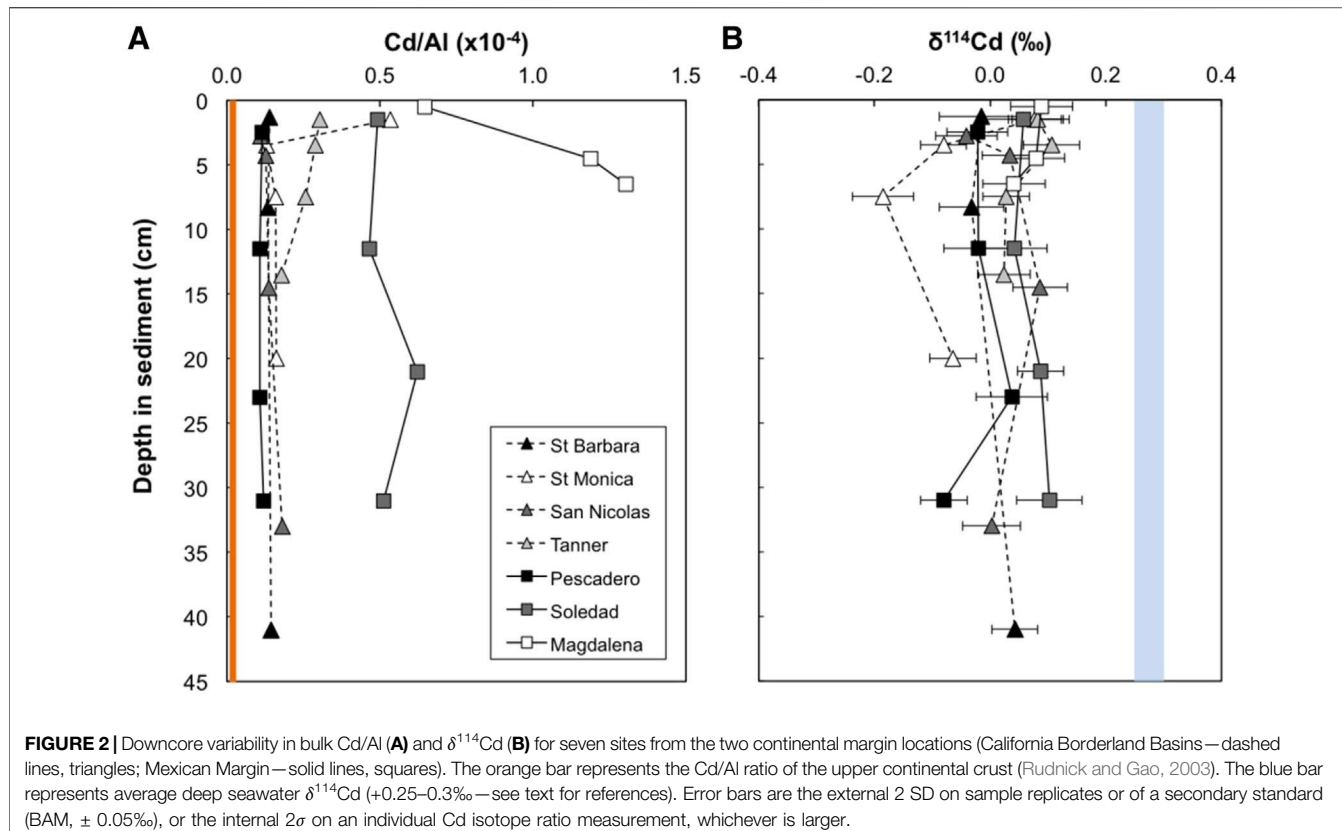


FIGURE 2 | Downcore variability in bulk Cd/Al (A) and $\delta^{114}\text{Cd}$ (B) for seven sites from the two continental margin locations (California Borderland Basins—dashed lines, triangles; Mexican Margin—solid lines, squares). The orange bar represents the Cd/Al ratio of the upper continental crust (Rudnick and Gao, 2003). The blue bar represents average deep seawater $\delta^{114}\text{Cd}$ (+0.25–0.3‰—see text for references). Error bars are the external 2 SD on sample replicates or of a secondary standard (BAM, $\pm 0.05\text{\textperthousand}$), or the internal 2σ on an individual Cd isotope ratio measurement, whichever is larger.

deviation variation over the entire sediment core), which is similar to the least reducing site, San Nicolas ($+0.02 \pm 0.05\text{\textperthousand}$), and within analytical uncertainty of the Tanner Basin ($+0.06 \pm 0.04\text{\textperthousand}$). The isotopic compositions of the Mexican margin sites are similar to the Borderland Basins, with average $\delta^{114}\text{Cd}$ values of $+0.07 \pm 0.03\text{\textperthousand}$ at both the Magdalena margin and Soledad Basin, and $0.00 \pm 0.06\text{\textperthousand}$ at the Pescadero slope. With the exception of Santa Monica, there are no analytically significant differences or discernible trends in $\delta^{114}\text{Cd}$ values with sediment depth. Santa Monica has a higher $\delta^{114}\text{Cd}$ value ($+0.08\text{\textperthousand}$) at the surface and lower values, to a minimum of $-0.19\text{\textperthousand}$, at depth. Excluding the surface-most sample, Santa Monica has the lowest average downcore $\delta^{114}\text{Cd}_{>1.5\text{cm}}$ value of $-0.11 \pm 0.07\text{\textperthousand}$.

Porewater Data

Porewater data and references for previously published sites are presented in Figure 3 and Supplementary Table 2. Data for previously unpublished sites, Santa Barbara and San Nicolas Basin will be briefly described here. Santa Barbara exhibits Fe-rich porewaters at the surface and reaches a peak of $185.2\text{ }\mu\text{M}$ in the top 2 cm of the sediment core. Dissolved Fe concentrations then decrease rapidly reaching $\sim 30\text{ }\mu\text{M}$ at 10 cm depth. Ammonia porewater concentrations steadily increase from 46 to $230\text{ }\mu\text{M}$ with depth, however there is a peak of $220\text{ }\mu\text{M}$ at a depth of 5.5 cm. San Nicolas has Fe–Mn rich porewaters and a porewater profile is presented in Figure 3C. Surface dissolved Mn and Fe

concentrations increase rapidly from near zero at the surface to a peak of 134.6 and $\sim 12\text{ }\mu\text{M}$ in the top 5 cm. Dissolved ammonia steadily increases from $\sim 0\text{ }\mu\text{M}$ at the surface to a maximum $\sim 70\text{ }\mu\text{M}$ at a depth of 20 cm. Sulphide porewater concentrations were below detection in both cores.

DISCUSSION

Minor Lithogenic Cd in Organic-Rich Sediments

The lithogenic Cd (Cd_{lith}) and bioauthigenic Cd concentrations (Cd_{auth}) can be estimated by using sample Al concentrations (Al_{bulk}) as a proxy for the detrital aluminosilicate fraction, as follows:

$$\text{Cd}_{\text{lith}} = \text{Cd}/\text{Al}_{\text{UCC}} \times \text{Al}_{\text{bulk}} \quad (2)$$

$$\text{Cd}_{\text{auth}} = \text{Cd}_{\text{bulk}} - \text{Cd}_{\text{lith}} \quad (3)$$

Assuming a lithogenic endmember similar to upper continental crust (UCC), with $\text{Cd}/\text{Al}_{\text{UCC}} = 0.011 \times 10^{-4}$ (Rudnick and Gao, 2003), lithogenic Cd accounts for a maximum of 10% of the total sample Cd in our samples (Supplementary Table 1). We can then correct bulk $\delta^{114}\text{Cd}$ values ($\delta^{114}\text{Cd}_{\text{bulk}}$) for this lithogenic contribution by assuming a $\delta^{114}\text{Cd}_{\text{lith}}$ value of $\sim 0\text{\textperthousand}$ (Schmitt et al., 2009; Lambelet et al., 2013), as follows:

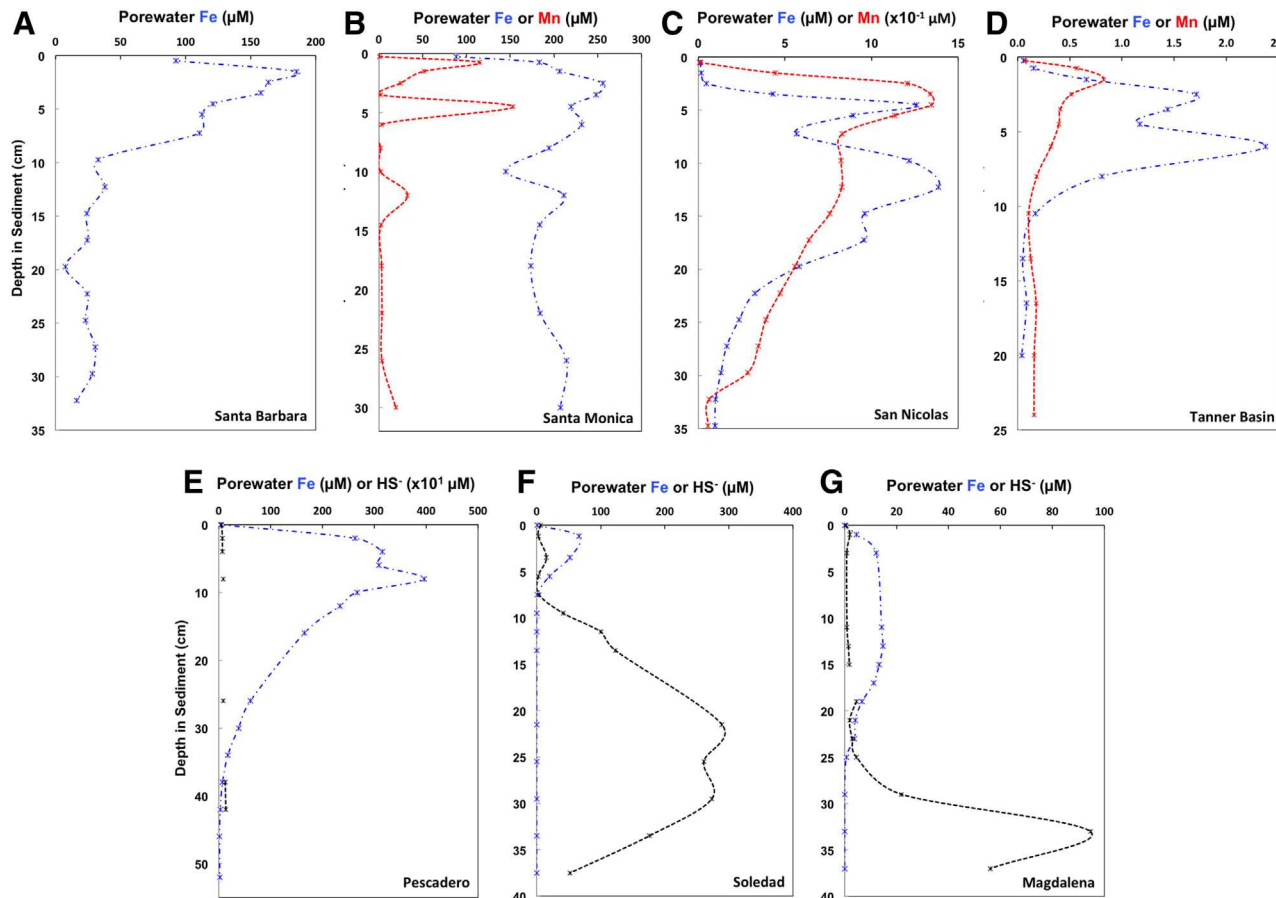


FIGURE 3 | Porewater Fe (blue dash-dot lines), Mn (red dashed lines) and HS⁻ (black dashed lines) concentrations for seven sites from the two continental margin locations, the California Borderland Basins (**A**—Santa Barbara, **B**—Santa Monica, **C**—San Nicolas, **D**—Tanner Basin) and the Mexican margin (**E**—Soledad Basin, **F**—Pescadero slope, **G**—Magdalena margin). Values and references are shown in **Supplementary Table 2**.

$$\delta^{114}\text{Cd}_{\text{auth}} = (\delta^{114}\text{Cd}_{\text{bulk}} \times \text{Cd}_{\text{bulk}} - \delta^{114}\text{Cd}_{\text{lith}} \times \text{Cd}_{\text{lith}}) / \text{Cd}_{\text{auth}} \quad (4)$$

in doing so, all calculated $\delta^{114}\text{Cd}_{\text{auth}}$ values (i.e., bioauthigenic Cd isotope compositions) are identical to or within analytical uncertainty of $\delta^{114}\text{Cd}_{\text{bulk}}$ values (**Supplementary Table 1**). Thus, we conclude that the influence of lithogenic Cd on our measured Cd isotope compositions is negligible, and bulk sedimentary $\delta^{114}\text{Cd}$ values are considered to represent the bioauthigenic Cd isotope composition (as reported in **Table 2**).

The key finding of this study is that bioauthigenic Cd in organic-rich continental margin sediments has a light isotopic composition, of 0 to +0.1‰, compared to global deep seawater, at about +0.3‰ (**Figure 2; Table 2**). Though we lack dissolved phase Cd isotope compositions for the local overlying water column at each site, deep water below the sill depth in the San Pedro Basin, which is an adjacent basin to Santa Monica, has an isotopic composition of +0.3‰, similar to the global deep water average of about +0.3‰ (Conway and John, 2015b); we assume that the deep water Cd isotope composition at our sites is similar.

The observed light Cd isotope composition of organic-rich sediments could reflect either (a) isotope fractionation during diagenesis or (b) an isotopically light particulate source of bioauthigenic Cd.

Limited Cd Isotope Fractionation During Diagenesis in Continental Margin Settings

During oxic diagenesis, it is well-documented that Cd is released to porewaters during remineralization of organic matter (e.g., Klinkhammer et al., 1982; Gobeil et al., 1987; McCorkle and Klinkhammer, 1991; Audry et al., 2006). In suboxic settings, where porewaters contain negligible dissolved oxygen and sulphide, near surface porewater Cd maxima are followed by strong depletion to low Cd concentrations (~0.1 nM) below, reflecting Cd release from organic matter followed by its near quantitative removal to an insoluble authigenic phase (Gobeil et al., 1987; McCorkle and Klinkhammer, 1991). Solid phase authigenic Cd enrichment is subsequently observed at the oxic/suboxic boundary (Rosenthal et al., 1995). Precipitation of authigenic CdS has been invoked to explain the observed Cd

removal in suboxic settings; due to its low sulphide solubility, Cd has a strong tendency to form insoluble sulphides in the presence of trace H₂S (e.g., Elderfield et al., 1981; Westerlund et al., 1986; Jacobs et al., 1987; Rosenthal et al., 1995; Morse and Luther, 1999).

In the anoxic and sulphidic porewaters of Narragansett Bay, Elderfield et al. (1981) found no detectable Cd (<0.5 nM), and also argued for precipitation of CdS (Elderfield, 1981; Elderfield et al., 1981). However, elevated porewater Cd (up to 2 nM) have been observed in strongly sulphidic porewaters of the Peru margin (up to several hundred μ M H₂S; Plass et al., 2020). Similarly, porewater Cd concentrations in sediments from the Laurentian Trough decreased to near zero in the suboxic zone, but increased again at depth in the anoxic zone (Gobeil et al., 1987). These observations suggest redissolution of authigenic CdS phases in highly sulphidic environments through the formation of bisulphide or polysulphide complexes (Gobeil et al., 1987; Plass et al., 2020).

In the absence of porewater Cd concentration data, we cannot conclusively evaluate the depth and degree of Cd removal to the solid phase. We note, however, that only one site (Soledad Basin) is strongly sulphidic at depths that overlap those of our sampling (Figures 2, 3), with resultant possible remobilization of CdS as bisulphide or polysulphide complexes. We also observe only muted variations in solid phase $\delta^{114}\text{Cd}$ and Cd concentrations with depth at all sites, including the Soledad Basin. Further studies coupling porewater and solid phase Cd isotope analysis are required to fully investigate the potential for Cd isotope fractionation during diagenesis. However, our dataset suggests very limited fractionation in reducing continental margin settings, with sedimentary isotopic compositions instead reflecting those of the Cd source(s).

Sources of Isotopically Light Bioauthigenic Cd

In the likely absence of diagenetic isotope fractionation, the relatively light Cd isotope composition of continental margin sediments must reflect an isotopically light water column source (or sources). We consider the following possible sources of bioauthigenic Cd to continental margin sediments: (1) organic matter (Elderfield et al., 1981; Rosenthal et al., 1995; Little et al., 2015), (2) CdS particulates (e.g., Janssen et al., 2014; Conway and John, 2015a; Bianchi et al., 2018; Xie et al., 2019a; Plass et al., 2020), and (3) Fe-oxyhydroxides (Klevenz et al., 2011; Conway and John, 2015a; Lee et al., 2018).

Organic Matter

Phytoplankton take up Cd in culture, and they take up more Cd when it is present at higher concentrations in the media (e.g. Sunda and Huntsman, 1998; Sunda and Huntsman, 2000). Increased uptake of Cd also occurs when stressed by low levels of other bioactive metals like Fe and Zn (Sunda and Huntsman, 2000; Cullen et al., 2003; Xu et al., 2007). Therefore, organic matter is likely to be an important vector transporting Cd to sediments, an assertion that is supported by the positive correlation observed between organic C and Cd/Al ratios in the sediments from this study (Figure 4A).

Plass et al. (2020) estimate the proportion of Cd delivered to sediment by organic matter for sites above, within and below the Peruvian ODZ by multiplying organic carbon accumulation rates by the Cd:C ratio in ‘average’ phytoplankton (i.e., Cd:P ratio of 0.21 mmol/mol, converted to Cd:C assuming a Redfield C:P ratio of 124:1; Ho et al., 2003; Moore et al., 2013). However, cellular Cd quotas vary widely, with Cd:P ratios in bulk particles from open and coastal ocean sites ranging from 0.04 to 2.3 mmol/mol (Martin and Knauer, 1973; Martin et al., 1976; Collier and Edmond, 1984; Kuss and Kremling, 1999; Ohnemus et al., 2016; Bourne et al., 2018; Lee et al., 2018; Black et al., 2019).

Bourne et al. (2018) present the most comprehensive dataset of directly measured particulate Cd:P ratios to date. They find distinct biogeographic and seasonal differences, and higher ratios in HNLC (high nutrient low chlorophyll) zones compared to oligotrophic gyres (Bourne et al., 2018). Although the sites in this study are not open ocean HNLC regions, they are locations of coastal upwelling in the northeast Pacific, and may therefore be expected to exhibit higher than ‘average’ euphotic zone phytoplankton Cd:P ratios (i.e., 0.21 mmol/mol; Ho et al., 2003). The only water column Cd:P data (dissolved or particulate, to our knowledge) from any one of our study sites supports this prediction: the mean euphotic zone particulate Cd:P ratio from the Santa Barbara Basin is 0.67 mmol/mol (1.13 mmol/mol in the <51 μ m size fraction, 0.26 mmol/mol in the >51 μ m size fraction; Bourne et al., 2018). Elevated Cd:P at this site is consistent with the high particulate Cd:P measured in the eastern tropical south Pacific (Peru margin) and other HNLC regions (0.49 \pm 0.23; Bourne et al., 2018). Therefore, we estimate the proportion of Cd delivered by organic matter to sediments at our sites for a range of Cd:P ratios of 0.21–0.67 mmol/mol (Table 3; Figure 4B). The lower end of this range (i.e., average phytoplankton; Ho et al., 2003) predicts that organic matter can account for ~50% or more of the Cd at all sites, and for 100% of the Cd in the San Nicolas and Tanner basins, while the upper end of the range allows that all of the Cd at all sites can be delivered by organic matter. In summary, organic matter is likely the primary vector transporting Cd to the sediment in margin settings. But is this Cd isotopically light?

In culture, phytoplankton preferentially take up light Cd, with calculated $\Delta^{114}\text{Cd}_{\text{biomass-medium}} = -0.3$ to $-1.3\text{\textperthousand}$ (where $\Delta^{114}\text{Cd}_{\text{biomass-medium}} = \delta^{114}\text{Cd}_{\text{biomass}} - \delta^{114}\text{Cd}_{\text{medium}}$) (Lacan et al., 2006; Gault-Ringold, 2011; Horner et al., 2013; John and Conway, 2014). Biological uptake of isotopically light Cd is consistent with observations of isotopically heavy surface seawater (e.g., Lacan et al., 2006; Ripperger et al., 2007; Conway and John, 2015a; 2015b) and studies of suspended particulate matter from the surface ocean, which have also found particulate Cd isotope compositions that are generally isotopically lighter than the contemporaneous dissolved phase (Yang et al., 2015, 2018; Janssen et al., 2019). However, particulate $\delta^{114}\text{Cd}$ ($\text{p}\delta^{114}\text{Cd}$) values in the surface ocean vary widely in different locations (Yang et al., 2015, 2018; Janssen et al., 2019). The northwest Pacific and the South China Sea exhibit a large range of measured $\text{p}\delta^{114}\text{Cd}$ from -1.5 to $+0.5\text{\textperthousand}$ (>0.2 μ m size fraction) and -0.9 to $+0.7\text{\textperthousand}$ (10 to >150 μ m) respectively. Meanwhile, in the Northeast Pacific, small size fraction (0.8–51 μ m) particulates from the euphotic zone are more comparable to deep-water dissolved $\delta^{114}\text{Cd}$ values, in the range $+0.34$ to $+0.54\text{\textperthousand}$ (Janssens et al., 2019).

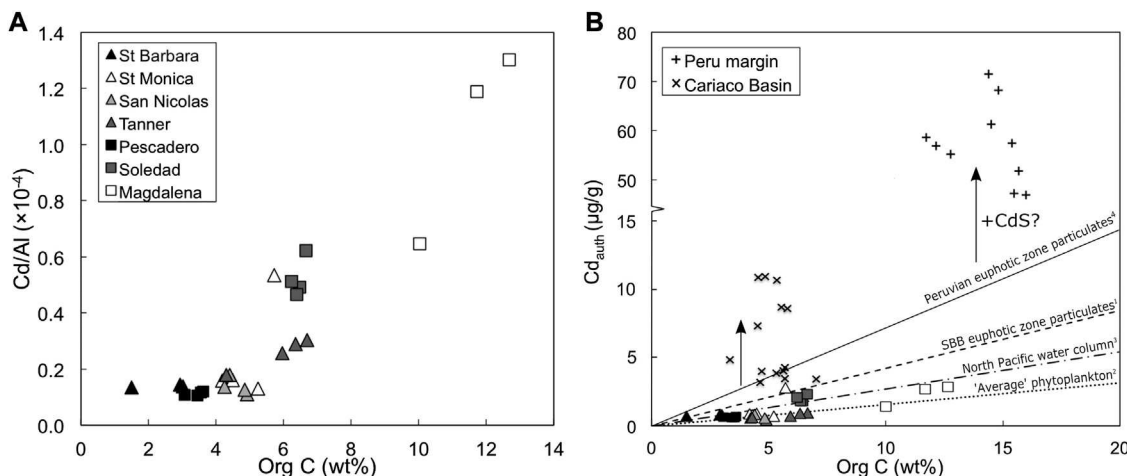


FIGURE 4 | (A) Positive covariation of sedimentary Cd/Al with organic carbon concentrations. **(B)** Bioauthigenic Cd_{auth} concentrations (Eq. 3) versus organic carbon concentrations for sediment samples in this study (triangles and squares) to sediments from the Peruvian ODZ (+) and the euxinic Cariaco Basin (x) (data: Little et al., 2015). For comparison, the dashed line gives the average Cd:C ratio from euphotic zone particles in the Santa Barbara Basin (1: Bourne et al., 2018), the dotted line shows Cd:C ratio in 'average' phytoplankton (2: Ho et al., 2003), the dot-dashed line shows the Cd:C ratio estimated for the North Pacific from an analysis of dissolved Cd and P concentration data (3: Quay et al., 2015), and the solid line shows the Cd:C ratio in euphotic zone particles from the Peru margin (4: 7.66×10^{-6} ; Bourne et al., 2018). Schematic vertical black arrows represent the proposed impact of CdS precipitation on sedimentary Cd_{auth} concentrations.

TABLE 3 | Calculated authigenic Cd (Eq. 3) and organic C mass accumulation rates, and estimated delivery of sedimentary Cd supplied by organic matter.

Site	Cd _{auth} ($\mu\text{g/g}$)	Cd _{auth} Mass accumulation rate ^a ($\mu\text{mol/m}^2/\text{yr}$)	Organic C accumulation rate ^a ($\text{mol/m}^2/\text{yr}$)	Range of Cd from organic matter ^b ($\mu\text{mol/m}^2/\text{yr}$)
Santa Barbara Basin	0.81	6.63	1.9	3.21–10.3
Santa Monica Basin	0.86	1.94	0.65	1.11–3.54
San Nicolas Basin	0.64	0.79	0.54	0.91–2.90
Tanner Basin	0.81	0.87	0.58	0.99–3.15
Pescadero slope	0.66	4.49	2.2	3.71–11.9
Soledad Basin	2.03	12.7	3.8	6.34–20.3
Magdalena margin	2.35	1.67	0.76	1.29–4.13

^aCalculated by multiplying mass accumulation rate shown in Table 1 by Cd or Organic C concentration (Table 2).

^bCalculated by multiplying organic C accumulation rate by molar Cd:C ratio of 1.69×10^{-6}

(min) and 5.4×10^{-6} (max) from Ho et al. (2003) and Bourne et al. (2018).

Sinking particles (>0.45 mm) from the South China Sea are isotopically heavier than suspended particles, at +0.8 to +2.8‰, and increase with increasing water depth (30–160 m; Yang et al., 2015). However, $\text{p}\delta^{114}\text{Cd}$ values were not measured at water depths >160 m, and it is uncertain whether these elevated sinking $\text{p}\delta^{114}\text{Cd}$ values are preserved deeper in the water column. Nevertheless, the authors hypothesize that the processes of microbial degradation/zooplankton repackaging preferentially decompose isotopically light Cd. In contrast, in the northeast Pacific, small size fraction (0.8–51 μm) $\text{p}\delta^{114}\text{Cd}$ values become more negative with depth (from 150 to 800 m), reaching a minimum of -0.5‰ (Janssen et al., 2019). In this case, the authors attribute the generation of a light signature either to isotope fractionation during remineralization of organic matter (but with the opposite sense to that proposed by Yang et al., 2015, i.e., preferential release of isotopically heavy Cd), or to the presence of multiple particulate Cd phases with variable

remineralization abilities (Janssen et al., 2019). It is possible that the light Cd isotope composition of these small size fraction particles is counterbalanced by an isotopically heavy Cd pool in large sinking particles, as observed in the South China Sea (Yang et al., 2015). Large size fraction particles were not analyzed in the northeast Pacific to test this hypothesis. Indeed, though the northeast Pacific small size fraction particles are isotopically lighter than the margin sediments reported herein – suggesting that they may contribute light Cd to the sediment – fast sinking, >50 μm particles are thought to be predominant in terms of mass flux to sediment (e.g., Clegg and Whitfield, 1990).

We conclude that organic matter is certainly a significant source of Cd to margin sediments, and may very well be isotopically light. However, further research is required to (a) better constrain the Cd isotope composition of diverse particulate

phases in the water column and (b) determine the extent to which the Cd isotope composition of organic-rich particles exported from the photic zone is preserved in sediments.

Cadmium Sulphide Precipitation

As discussed above, CdS phases sequester Cd in anoxic and suboxic sediments (e.g., Elderfield et al., 1981; Rosenthal et al., 1995) and precipitate within the water column of euxinic basins (e.g., Jacobs et al., 1985; Tankéré et al., 2001). It has also been hypothesized that CdS precipitation may occur in the open ocean, either in ODZs in reducing microenvironments within decomposing organic matter (Janssen et al., 2014; Conway and John, 2015a; Bianchi et al., 2018) and/or in bottom waters near the sediment-water interface along reducing continental margins (Xie et al., 2019b; Plass et al., 2020). This hitherto unrecognized water column sulphide sink of Cd may be an important flux in the global oceanic Cd budget (e.g., Janssen et al., 2014; Guinoiseau et al., 2019).

Mass balance calculations show evidence for an additional source of particulate Cd to sediments (beyond that supplied by organic matter) for the functionally anoxic Peru margin (Little et al., 2015; Plass et al., 2020) and the modern euxinic Cariaco Basin, where euxinic refers to the presence of free sulphide in the bottom water (Little et al., 2015). Indeed, dissolved Cd is quantitatively removed below the redoxcline in the Cariaco Basin (Jacobs et al., 1987). Authigenic Cd concentrations in Cariaco Basin and Peru margin sediments are significantly elevated above what is likely to be supplied by organic matter (Figure 4B). This enrichment is consistent with supply via CdS precipitation, and can be observed as a pseudo-vertical trend in organic C versus Cd_{auth} space (arrows, Figure 4B). Of the sites investigated in this study, the Soledad Basin and the Magdalena margin are the most reducing, with sulphidic porewaters (Chong et al., 2012), and these two sites are also the most enriched in Cd (Figure 4). Sediment samples from the Soledad Basin also show a near-vertical trend in organic C versus Cd_{auth} space (Figure 4B), albeit at much lower levels of overall Cd enrichment than, for example, the Peru margin (Figure 4B). It is therefore plausible that a small part of the Cd budget in the Soledad Basin and Magdalena margin sediments was supplied by CdS precipitation, if we assume a Cd:C ratio similar to average phytoplankton (Table 2; Ho et al., 2003).

Cadmium isotopes may facilitate the identification of a CdS source, because non-quantitative CdS precipitation is accompanied by light Cd isotope fractionation. In experiments, Guinoiseau et al. (2018) observed an isotope fractionation factor for CdS precipitation of $\Delta^{114}\text{Cd}_{\text{CdS-medium}} \approx -0.3\text{\textperthousand}$ (Guinoiseau et al., 2018), consistent with the light isotope composition of hydrothermal CdS precipitates (Schmitt et al., 2009). Dissolved Cd in the Mauritanian ODZ and the Angola Basin is depleted relative to P and is isotopically heavy (up to $1.3\text{\textperthousand}$; Janssen et al., 2014; Conway and John, 2015a; Guinoiseau et al., 2019), supporting the hypothesized precipitation of CdS within degrading organic matter in ODZs. Furthermore, the complementary particulate Cd pool from the Mauritanian ODZ is enriched relative to phosphate and is isotopically light (-0.01 to $+0.35\text{\textperthousand}$; Janssen et al., 2014)

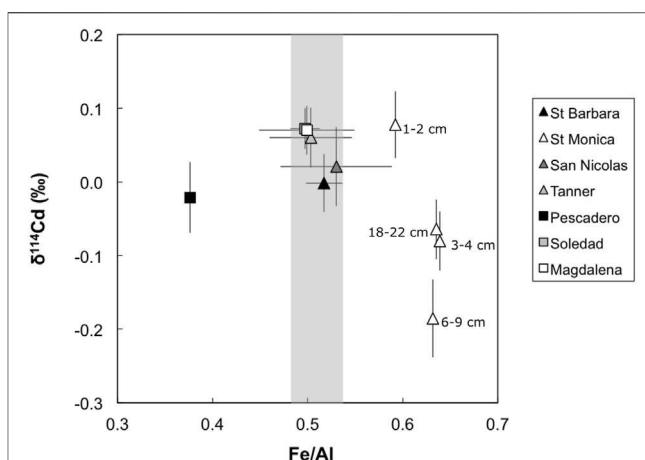


FIGURE 5 | Site-averaged bulk sediment Fe/Al vs. $\delta^{114}\text{Cd}$ values, except for Santa Monica where all data points are shown (white triangles). Shaded gray bar represents the Fe/Al ratio of the upper continental crust (UCC; Rudnick and Gao, 2003). Note that Fe/Al ratios are enriched at Santa Monica (and depleted at the Pescadero slope) compared to UCC. Error bars for site average are 1 standard deviation of the entire sediment column and error bars for Santa Monica are external 2 SD on sample replicates or of a secondary standard (BAM, $\pm 0.05\text{\textperthousand}$), or the internal 2σ on an individual Cd isotope ratio measurement, whichever is larger.

compared to average deep seawater. However, such evidence for CdS precipitation is not observed in all ODZs, including the North Pacific ODZ (Conway and John, 2015b; Janssen et al., 2017) and the open Peru margin ODZ (John et al., 2018; Xie et al., 2019b). The extent to which CdS precipitation occurs in ODZs, and the longevity of these particles as they sink through the water column to the sediment remain topics of ongoing research (Guinoiseau et al., 2019; de Souza et al., in review).

While organic-matter associated CdS precipitation in ODZs and potential burial in sediments remains a topic of contention, CdS precipitation in bottom waters overlying sulphidic continental margin sediments is supported by *in situ* benthic chamber incubations and water column Cd isotope analyses (Xie et al., 2019b; Plass et al., 2020). At sites within the Peruvian ODZ, Plass et al. (2020) report *in-situ* benthic chamber Cd fluxes into the sediment 25–40 times higher than calculated diffusive fluxes of dissolved Cd into the sediments (Plass et al., 2020). The authors suggest that leakage of trace H₂S into bottom waters from sediment porewaters leads to near seafloor CdS precipitation, thus explaining their observed high sedimentary Cd fluxes (Plass et al., 2020). We emphasize that this mechanism is distinct from the organic matter associated-CdS precipitation in the water column (e.g., Janssen et al., 2014; Bianchi et al., 2018). Consistent with near-seafloor CdS precipitation, Xie et al. (2019b) report strong dissolved Cd depletion and Cd isotope fractionation (dissolved $\delta^{114}\text{Cd}$ up to $+1.30\text{\textperthousand}$) associated with a sulphidic plume that covered much of the Peruvian continental shelf during January 2009 (Schunck et al., 2013). Their data suggest an isotope effect on CdS precipitation of $\Delta^{114}\text{Cd}_{\text{CdS-seawater}} = -0.29\text{\textperthousand}$,

comparable to the experimental estimate of Guinoiseau et al. (2018).

Iron Oxyhydroxides

The Santa Monica Basin samples have variable and generally lower $\delta^{114}\text{Cd}$ values (+0.08 to -0.19‰) compared to the other sites (**Figure 2**), although only the sample from 6–9 cm depth is analytically distinct (-0.19‰). Compared to the other sites Santa Monica Basin sediments have elevated solid phase Fe/Al ratios, which may be linked to the observed low $\delta^{114}\text{Cd}$ values (**Figure 5**). Iron enrichment in this setting is likely to originate from a form of open-marine Fe ‘shuttle’ (e.g., Scholz et al., 2014), whereby dissolved Fe (II) is released from reducing shelf sediments and then reprecipitated as Fe (III) oxyhydroxides coupled to microbial nitrate reduction in the ODZ (Scholz et al., 2016; Heller et al., 2017). Though Santa Monica porewaters are strongly ferruginous (McManus et al., 1997; 1998)—a diagenetic regime that would typically be reflected as a *source* of Fe(II) to the water column rather than a sink—solid phase Fe enrichment presumably reflects the basinal geography (e.g., Severmann et al., 2010), which traps Fe supplied to the deep basin via the redox shuttle. Given that there is evidence of deep sulphate reduction in porewaters, the absence of porewater sulphide in the upper sediment package is consistent with its rapid titration by the high concentrations of Fe (McManus et al., 1997; 1998). We note that sediments from the Pescadero slope, which also has strongly ferruginous porewaters (Chong et al., 2012), exhibits solid-phase Fe depletion (**Figure 5**), consistent with a benthic flux of Fe(II) into bottom waters in this unrestricted hydrographic setting.

Scavenging of Cd by Fe oxyhydroxides has been hypothesized previously; for example, it has been suggested that particulate Cd enrichment in the lower Peru margin ODZ is associated with Fe-oxyhydroxide phases (Lee et al., 2018). Such scavenging of Cd by Fe oxyhydroxides may enhance the supply of isotopically light Cd to the Santa Monica Basin.

To our knowledge, there has been no experimental work investigating Cd isotope fractionation during sorption to Fe oxyhydroxides, although it has been suggested that Fe oxyhydroxides may scavenge Cd as a CdS phase (Klevenz et al., 2011; Conway and John, 2015a), which, as discussed, would likely be isotopically light. Experimental sorption of Cd on Mn-oxides initially shows preference for light isotopes, though the magnitude of fractionation ($\Delta^{114}\text{Cd}_{\text{MnO}_2\text{-aqueous}} = \delta^{114}\text{Cd}_{\text{MnO}_2} - \delta^{114}\text{Cd}_{\text{aqueous}}$) declines from -0.8 to -0.2‰ over time (Wasylewski et al., 2014). In natural settings, Fe-Mn crusts record the Cd isotope composition of ambient seawater without fractionation (Schmitt et al., 2009; Horner et al., 2010). A thorough evaluation of the potential for an Fe redox shuttle influence on the Cd isotope composition of sediments awaits future studies investigating Cd isotope fractionation on sorption to Fe-oxyhydroxide phase, and data from other ferruginous sites like the Santa Monica Basin.

Implications for Cd Oceanic Mass Balance

The sedimentary Cd concentration and $\delta^{114}\text{Cd}$ data in this study allow us to place new constraints on the outputs of Cd from the

ocean and evaluate a recent estimate of the Cd sink driven by water column sulphide formation in the global oceanic Cd budget. Previous estimates of the major input and output fluxes are presented in **Table 4**, along with new estimates from this study.

The main Cd source to the oceans is the dissolved riverine flux, estimated at $0.4\text{--}2.7 \times 10^7 \text{ mol/yr}$ (van Geen et al., 1995; Gaillardet et al., 2003). The best estimate given in **Table 4** is the higher value from Gaillardet et al. (2003), because this study considers a larger compilation of rivers. Estimates of the natural mineral dust flux by van Geen et al. (1995) were made by reducing the total estimated aerosol flux by a factor of 10 to take the increase in anthropogenic emissions into account (Nriagu, 1980). The best estimate for the natural dust flux is thus $0.3 \times 10^7 \text{ mol/yr}$ (**Table 4**). The best guess isotopic compositions of the mineral dust and dissolved riverine sources of Cd are 0.0‰ and $+0.2 \pm 0.1\text{‰}$ respectively (Lambelet et al., 2013; Bridgestock et al., 2017). We note that this riverine isotopic composition is based on a single study reporting the Cd isotope composition of samples spanning the salinity gradient on the Siberian Shelf, and thus represents an average $\delta^{114}\text{Cd}$ value of the discharge of four Siberian rivers only.

We estimate the flux of Cd to continental margins delivered in association with organic matter by multiplying the estimated global organic carbon deposition on continental margins, of $15.6 \times 10^{12} \text{ mol/yr}$ (Jahnke, 2010), with a range of estimated Cd:C ratios in phytoplankton (discussed in “Organic Matter” section). For Cd:C ratios ranging from ‘average phytoplankton’, at 1.69×10^{-6} (Ho et al., 2003), to that of Peruvian euphotic zone particulates, at 7.66×10^{-6} (Bourne et al., 2018), we calculate an organic matter associated Cd flux to continental margin sediments of $2.6\text{--}12.0 \times 10^7 \text{ mol/yr}$. The minimum end of this range likely underestimates the Cd flux in upwelling regions, while the maximum estimate is probably too high, because such high Cd:C ratios are not observed on a global scale (section “Organic Matter”; Quay et al., 2015; Bourne et al., 2018). Instead, we suggest the export-flux-weighted phytoplankton Cd:C ratio (i.e., the average Cd:C ratio of organic matter that is exported from the photic zone globally) is likely to be close to the average upwelling (HNLC) Cd:C ratio of 3.95×10^{-6} (or a Cd:P ratio of 0.49 mmol/mol; Bourne et al., 2018). This is because upwelling regions have high sinking particulate fluxes. Hence, we make a best estimate for global organic matter associated Cd flux of $6.2 \times 10^7 \text{ mol/yr}$.

We suggest that CdS precipitation is likely a rather minor contributor to sedimentary Cd fluxes globally, albeit locally significant (e.g., in the core of the Peruvian ODZ; Little et al., 2015; Plass et al., 2020). This conclusion contrasts with a recent estimation of the global water column CdS sink, at $0.87\text{--}104 \times 10^7 \text{ mol/yr}$ (Guinouseau et al., 2019), based on the optimized particle cycling model of Bianchi et al. (2018). The large range derived by these authors is due to the uncertainty in the dissolution rate of CdS particles in seawater. The maximum estimate is two orders of magnitude greater than the total known inputs to the ocean, and eight times our maximum estimated continental margin sink ($12.0 \times 10^7 \text{ mol/yr}$; **Table 4**). Thus, we conclude that the global Cd sink resulting from water-column CdS formation is likely to be

TABLE 4 | Oceanic Mass Balance of Cd from published data and data presented in this study.

	Mass ocean (kg)	Mass Cd (mol)		References	
Global oceans	1.3521×10^{21}	8.36×10^{11}		1	
Input fluxes	Cd flux range ($\times 10^7$ mol/yr)	Cd flux best estimate ($\times 10^7$ mol/yr)	$\delta^{114}\text{Cd}$ range (‰)	$\delta^{114}\text{Cd}$ best estimate (‰)	
Rivers	0.4–2.7	2.7	+0.1 – +0.3	+0.2	2
Dust	0.2–0.4	0.3	-0.2 – +0.2	0.0	2
Hydrothermal	(0.2–2.6)	n			3
Total	0.6–3.8	3.0	+0.0 – +0.3	+0.2	
Output fluxes	Cd flux range ($\times 10^7$ mol/yr)	Cd flux best estimate ($\times 10^7$ mol/yr)	$\delta^{114}\text{Cd}$ range (‰)	$\delta^{114}\text{Cd}$ best estimate (‰)	
Oxic sediments	n	n	+0.3 – +0.4	+0.3	4
Continental margins^a	2.6–12.0	6.2	-0.2 – +0.1	0.0	5
Euxinic	n	n			6
Hydrothermal	(0.2–2.6)				3
Total sink	2.6–12.0	6.2	-0.2 – +0.1	0.0	
Residence time (kyrs)	7–32				
	13.5				

Values in parentheses are assumed to be removed quantitatively close to the source and therefore not included in the total mass balance. Values in bold are data presented from this study.

^aContinental margins include suboxic and anoxic conditions and basin settings.

n—negligible.

References: 1. Baumgartner and Reichel (1975); Chester and Jickells (2012) 2. van Geen et al. (1995); Gaillardet et al. (2003); Lambelet et al. (2013); Bridgestock et al. (2017); 3. Von Damm et al., 1985; 4. Schmitt et al. (2009); Horner et al. (2010); 5. van Geen et al. (1995); Morford and Emerson (1999); Little et al. (2015); This study. 6. Little et al. (2015).

at the lower end of the model-based estimate of Guinoseau et al. (2019).

The concentration-weighted average $\delta^{114}\text{Cd}$ of the organic-rich sediments analyzed in this study is +0.04‰. This value is similar to the estimated Cd isotope compositions of the mineral dust and riverine input fluxes (~0 and ~0.2‰ respectively) (Lambelet et al., 2013; Bridgestock et al., 2017), suggesting that the isotope compositions of the Cd input and output fluxes are approximately balanced. However, our current best estimate of the Cd output flux to sediments is two times larger than the known input fluxes.

To account for this mass imbalance, either the known inputs are underestimated or there remain unrecognized sources of Cd to the ocean. One possible additional input of Cd to the oceans is partial mobilization from riverine particulates in estuaries (as recently suggested for several trace elements: e.g., Jones et al., 2014; Little et al., 2017). Several studies indicate that Cd can behave non-conservatively in estuarine systems (e.g., Elbaz-Poulichet et al., 1987; Comans and Vandijk, 1988; Elbaz-Poulichet et al., 1996; Waeles et al., 2004; Waeles et al., 2005; Lambelet et al., 2013). The mixing of freshwater and saltwater alters the speciation of Cd through the formation of soluble chloro complexes, which can drive the dissolution of particulate Cd (e.g., Elbaz-Poulichet et al., 1987). Particulate riverine Cd fluxes, estimated at 2.05×10^8 mol/yr, are an order of magnitude higher than dissolved fluxes (Gaillardet et al., 2003). Therefore, partial dissolution of

riverine particulates, likely with a lithogenic Cd isotope composition (~0‰), could account for the existing flux imbalance.

Conclusion and Outlook for Cd Isotopes as a Proxy

It has been suggested that Cd isotopes may be a useful tracer of past ocean productivity (e.g., Georgiev et al., 2015). Conceptually, an isotopic tracer of productivity (or, more accurately, of nutrient utilization) requires three ingredients:

- (1) Isotopic fractionation on biological uptake, which is quantifiable and consistent, e.g., through culturing studies (e.g., Lacan et al., 2006).
- (2) Translation of this biological uptake-driven isotope fractionation into observations in the ‘real world’, i.e., the degree of surface ocean isotopic fractionation should be proportional to the extent of Cd removal into particles (e.g., Ripperger et al., 2007).
- (3) Sedimentary archive(s) of either (a) the residual, fractionated surface ocean (e.g., carbonates; Hohl et al., 2017) and/or (b) the cumulative solid phase, i.e., organic matter (e.g., Georgiev et al., 2015). In addition, an archive of the contemporaneous nutrient ‘source’ (often assumed to be the deep ocean) is required to make quantitative estimates of nutrient utilization (e.g., Fe-Mn crusts; Schmitt et al., 2009; Horner et al., 2010).

In this study, we consider the question: do organic-rich sediments record the isotopic composition of the organic matter exported from the surface ocean? We find that, in sites without the build-up of HS^- in porewaters close to the sediment-water interface, organic matter is the primary source of Cd to margin sediments. In addition, bioauthigenic Cd in organic-rich sediments is isotopically light, consistent with preferential uptake of light isotopes by primary producers. These two first-order findings suggest that Cd isotope compositions in organic-rich sediments do hold promise as a tracer of nutrient utilisation.

However, there are several caveats to this simple interpretation of Cd and Cd isotopes in organic-rich sediments. First, we find that water column CdS precipitation provides a second possible isotopically light source of Cd to sediments, which in the most reducing settings may account for a significant fraction of the Cd budget (e.g., Plass et al., 2020). Scavenging by Fe oxyhydroxides may provide a third isotopically light flux of Cd to sediments. There is no straightforward means to differentiate isotopically light Cd sourced from organic matter and that from water column CdS precipitation (or scavenged by Fe oxyhydroxides).

Second, it is classically assumed that biological uptake in the surface ocean follows a closed-system Rayleigh fractionation model. This model describes Cd isotope systematics quite well in nutrient-rich regions (e.g., Abouchami et al., 2011; Xue et al., 2013; Abouchami et al., 2014; Janssen et al., 2017; Yang et al., 2018), but not in Cd-poor regions, with explanations for non-Rayleigh behavior including open system steady-state, buffering by organic ligands, external Cd sources, or species-specific Cd isotope fractionation factors (Gault-Ringold et al., 2012; Xie et al., 2017; 2019a; Janssen et al., 2017; George et al., 2019; Sieber et al., 2019a; 2019b). This complexity in the dissolved phase is matched by the variable particulate Cd isotope compositions measured to date, which also preclude straightforward interpretation (**Organic matter**; Janssen et al., 2014; 2019; Yang et al., 2015; 2018).

Third, our studied sites have substantially different organic carbon burial rates (**Table 1**) yet similar Cd isotope compositions, suggesting that sedimentary $\delta^{114}\text{Cd}$ values may not correlate directly with overlying productivity. Only a tiny fraction (<1%) of the organic matter produced in the surface ocean is ultimately preserved in continental margin sediments (e.g., Hedges and Keil, 1995) and the links between export production and sedimentary metal concentrations and isotopic compositions remains an area of active research. Remineralization, for example, is suggested to preferentially release heavy Cd in the modern northeast Pacific, providing another pathway to the generation of isotopically light Cd in sediments (Janssen et al., 2019). We note that the opposite sense of fractionation on remineralization (i.e., preferential release of light Cd) has been proposed based on particulate Cd isotope compositions from the South China Sea (Yang et al., 2015).

To conclude, the degree to which $\delta^{114}\text{Cd}$ values in underlying organic-rich sediments truly reflect surface ocean nutrient utilization remains uncertain, due to the complex processes

that govern Cd isotope fractionation in the water column and the possibility of a water column CdS flux. A recent study of Cd isotope compositions in organic-rich sediments spanning from the Upper Cretaceous (including Oceanic Anoxic Event 2) places similar emphasis on the role of local redox rather than productivity changes in controlling the range of observed sedimentary $\delta^{114}\text{Cd}$ values (Sweere et al., 2020). In agreement with that study, we recommend that researchers exercise considerable caution if interpreting Cd isotope compositions in ancient organic-rich sediments as solely reflecting changes in past ocean productivity.

DATA AVAILABILITY STATEMENT

The original contributions presented in the study are included in the article/**Supplementary material**, further inquiries can be directed to the corresponding author.

AUTHOR CONTRIBUTIONS

JM and SS collected sediment and porewater samples, and also conducted element porewater analyses. LC, KK and SHL prepared the samples for isotopic analysis and conducted isotopic measurements. LC and SHL wrote the manuscript with inputs from all authors.

FUNDING

SHL acknowledges financial support from the Natural Environment Research Council (NE/P018181/2). JM's contributions were supported by NSF grants OCE-0219651 and OCE-1657832. SS's contributions were supported by NSF grant OC-1657832

ACKNOWLEDGMENTS

We would like to thank two reviewers and the editor Susann Henkel for comments that significantly improved the manuscript. We thank the MAGIC group at Imperial College London for the support and smooth running of the laboratories. We are also grateful for several helpful discussions with Tristan Horner during the project and would also like to thank Gregory de Souza for feedback on an earlier version of the manuscript.

SUPPLEMENTARY MATERIAL

The supplementary Material for this article can be found online at: <https://www.frontiersin.org/articles/10.3389/feart.2021.623720/full#supplementary-material>.

REFERENCES

Abouchami, W., Galer, S. J. G., de Baar, H. J. W., Alderkamp, A. C., Middag, R., Laan, P., et al. (2011). Modulation of the Southern Ocean cadmium isotope signature by ocean circulation and primary productivity. *Earth Planet. Sci. Lett.* 305, 83–91. doi:10.1016/j.epsl.2011.02.044

Abouchami, W., Galer, S. J. G., de Baar, H. J. W., Middag, R., Vance, D., Zhao, Y., et al. (2014). Biogeochemical cycling of cadmium isotopes in the southern ocean along the zero meridian. *Geochimica et Cosmochimica Acta* 127, 348–367. doi:10.1016/j.gca.2013.10.022

Audry, S., Blanc, G., Schäfer, J., Chaillou, G., and Robert, S. (2006). Early diagenesis of trace metals (Cd, Cu, Co, Ni, U, Mo, and V) in the freshwater reaches of a macrotidal estuary. *Geochimica et Cosmochimica Acta* 70, 2264–2282. doi:10.1016/j.gca.2006.02.001

Baumgartner, A., and Reichel, E. (1975). The world water balance. Amsterdam: Elsevier

Berelson, W. M., Prokopenko, M., Sansone, F. J., Graham, A. W., McManus, J., and Bernhard, J. M. (2005). Anaerobic diagenesis of silica and carbon in continental margin sediments: discrete zones of TCO₂ production. *Geochimica et Cosmochimica Acta* 69, 4611–4629. doi:10.1016/j.gca.2005.05.011

Bianchi, D., Weber, T. S., Kiko, R., and Deutsch, C. (2018). Global niche of marine anaerobic metabolisms expanded by particle microenvironments. *Nat. Geosci.* 11, 263–268. doi:10.1038/s41561-018-0081-0

Black, E. E., Lam, P. J., Lee, J. M., and Buesseler, K. O. (2019). Insights from the 238U–234Th method into the coupling of biological export and the cycling of cadmium, cobalt, and manganese in the southeast pacific ocean. *Glob. Biogeochem. Cycles* 33, 15–36. doi:10.1029/2018GB005985

Bourne, H. L., Bishop, J. K. B., Lam, P. J., and Ohnemus, D. C. (2018). Global spatial and temporal variation of Cd:P in euphotic zone particulates. *Glob. Biogeochem. Cycles* 32, 1123–1141. doi:10.1029/2017gb005842

Boyle, E. A., Sclater, F., and Edmond, J. M. (1976). On the marine geochemistry of cadmium. *Nature* 263, 42–44. doi:10.1038/263042a0

Bralower, T. J., and Thierstein, H. R. (1987). Organic carbon and metal accumulation rates in Holocene and mid-Cretaceous sediments: palaeoceanographic significance. *Geol. Soc. Lond. Spec. Publications* 26, 345–369. doi:10.1144/gsl.sp.1987.026.01.23

Brand, L. E., Sunda, W. G., and Guillard, R. R. L. (1986). Reduction of marine phytoplankton reproduction rates by copper and cadmium. *J. Exp. Mar. Biol. Ecol.* 96, 225–250. doi:10.1016/0022-0981(86)90205-4

Bridgestock, L., Rehkämper, M., van de Flierdt, T., Murphy, K., Khondoker, R., Baker, A. R., et al. (2017). The Cd isotope composition of atmospheric aerosols from the Tropical Atlantic Ocean. *Geophys. Res. Lett.* 44, 2932–2940. doi:10.1002/2017gl072748

Bruland, K. W., Middag, R., and Lohan, M. C. (2014). Controls of trace metals in Seawater. H.D. Holland, K.K. Turekian (oxford, elsevier). *Treatise Geochem.* 14, 19–51. doi:10.1016/b978-0-08-095975-7.00602-1

Bruland, K. W. (1980). Oceanographic distributions of cadmium, zinc, nickel, and copper in the North Pacific. *Earth Planet. Sci. Lett.* 47, 176–198. doi:10.1016/0012-821x(80)90035-7

Bruland, K. W., Orians, K. J., and Cowen, J. P. (1994). Reactive trace metals in the stratified central North Pacific. *Geochimica et Cosmochimica Acta* 58, 3171–3182. doi:10.1016/0016-7037(94)90044-2

Chester, R., and Jickells, T. (2012). *Marine geochemistry 3rd ed.* London: Wiley-Blackwell. doi:10.1002/9781118349083

Chong, L. S., Prokopenko, M. G., Berelson, W. M., Townsend-Small, A., and McManus, J. (2012). Nitrogen cycling within suboxic and anoxic sediments from the continental margin of Western North America. *Mar. Chem.* 128–129, 13–25. doi:10.1016/j.marchem.2011.10.007

Clegg, S. L., and Whitfield, M. (1990). A generalized model for the scavenging of trace metals in the open ocean-I. Particle cycling. *Deep Sea Res. A. Oceanogr. Res. Pap.* 37, 809–832. doi:10.1016/0198-0149(90)90008-j

Collier, R., and Edmond, J. (1984). The trace element geochemistry of marine biogenic particulate matter. *Prog. Oceanogr.* 13, 113–199. doi:10.1016/0079-6611(84)90008-9

Conway, T. M., and John, S. G. (2015a). Biogeochemical cycling of cadmium isotopes along a high-resolution section through the North Atlantic Ocean. *Geochimica et Cosmochimica Acta* 148, 269–283. doi:10.1016/j.gca.2014.09.032

Conway, T. M., and John, S. G. (2015b). The cycling of iron, zinc and cadmium in the North East Pacific Ocean - insights from stable isotopes. *Geochimica et Cosmochimica Acta* 164, 262–283. doi:10.1016/j.gca.2015.05.023

Cullen, J. T., Chase, Z., Coale, K. H., Fitzwater, S. E., and Sherrell, R. M. (2003). Effect of iron limitation on the cadmium to phosphorus ratio of natural phytoplankton assemblages from the Southern Ocean. *Limnol. Oceanogr.* 48, 1079–1087. doi:10.4319/lo.2003.48.3.1079

Cullen, J., and Maldonado, M. (2012). “Biogeochemistry of Cadmium and Its Release to the Environment,” in *Cadmium: From Toxicity to Essentiality*, Editors A. Sigel, H. Sigel, and R. Sigel (Dordrecht: Springer), 31–62. doi:10.1007/978-94-007-5179-2

Elbaz-Poulichet, F., Martin, J. M., Huang, W. W., and Zhu, J. X. (1987). Dissolved Cd behaviour in some selected French and Chinese estuaries. Consequences on Cd supply to the ocean. *Mar. Chem.* 22, 125–136. doi:10.1016/0304-4203(87)90004-1

Elbaz-Poulichet, F. c., Garnier, J.-M., Guan, D. M., Martin, J.-M., and Thomas, A. J. (1996). The conservative behaviour of trace metals (Cd, Cu, Ni and Pb) and as in the surface plume of stratified estuaries: example of the Rhône river (France). *Estuarine, Coastal Shelf Sci.* 42, 289–310. doi:10.1006/ecss.1996.0021

Elderfield, H., McCaffrey, R. J., Luedtke, N., Bender, M., and Truesdale, V. W. (1981). Chemical diagenesis in Narragansett Bay sediments. *Am. J. Sci.* 281, 1021–1055. doi:10.2475/ajs.281.8.1021

Elderfield, H. (1981). Metal-organic associations in interstitial waters of Narragansett Bay sediments. *Am. J. Sci.* 281, 1184–1196. doi:10.2475/ajs.281.9.1184

Emery, K. O. (1960). Basin plains and aprons off southern California. *J. Geol.* 68, 464–479. doi:10.1086/626678

Finney, B. P., and Huh, C. A. (1989). History of metal pollution in the Southern California Bight: an update. *Environ. Sci. Technol.* 23, 294–303. doi:10.1021/es00180a005

Gaillardet, J., Viers, J., and Dupré, B. (2003). “Trace elements in river waters,” in *Treatise on Geochemistry*. Editors D. H. Heinrich, and Karl, K. T. (Oxford: Elsevier), 225–272. doi:10.1016/b0-08-043751-6/05165-3

Gault-Ringold, M. (2011). *The marine biogeochemistry of cadmium: studies of cadmium isotopic variations in the southern ocean (thesis, doctor of philosophy)*. Dunedin: University of Otago.

Gault-Ringold, M., Adu, T., Stirling, C. H., Frew, R. D., and Hunter, K. A. (2012). Anomalous biogeochemical behavior of cadmium in subantarctic surface waters: mechanistic constraints from cadmium isotopes. *Earth Planet. Sci. Lett.* 341–344, 94–103. doi:10.1016/j.epsl.2012.06.005

George, E., Stirling, C. H., Gault-Ringold, M., Ellwood, M. J., and Middag, R. (2019). Marine biogeochemical cycling of cadmium and cadmium isotopes in the extreme nutrient-depleted subtropical gyre of the South West Pacific Ocean. *Earth Planet. Sci. Lett.* 514, 84–95. doi:10.1016/j.epsl.2019.02.031

Georgiev, S. V., Horner, T. J., Stein, H. J., Hannah, J. L., Bingen, B., and Rehkämper, M. (2015). Cadmium-isotopic evidence for increasing primary productivity during the Late Permian anoxic event. *Earth Planet. Sci. Lett.* 410, 84–96. doi:10.1016/j.epsl.2014.11.010

Gobeil, C., Silverberg, N., Sundby, B., and Cossa, D. (1987). Cadmium diagenesis in Laurentian Trough sediments. *Geochimica et Cosmochimica Acta* 51, 589–596. doi:10.1016/0016-7037(87)90071-8

Guinoiseau, D., Galer, S. J. G., and Abouchami, W. (2018). Effect of cadmium sulphide precipitation on the partitioning of Cd isotopes: implications for the oceanic Cd cycle. *Earth Planet. Sci. Lett.* 498, 300–308. doi:10.1016/j.epsl.2018.06.039

Guinoiseau, D., Galer, S. J. G., Abouchami, W., Frank, M., Achterberg, E. P., and Haug, G. H. (2019). Importance of cadmium sulfides for biogeochemical cycling of Cd and its isotopes in oxygen deficient zones-A case study of the Angola basin. *Glob. Biogeochem. Cycles* 33, 1746–1763. doi:10.1029/2019gb006323

Hedges, J. I., and Keil, R. G. (1995). Sedimentary organic matter preservation: an assessment and speculative synthesis. *Mar. Chem.* 49, 81–115. doi:10.1016/0304-4203(95)00008-F

Heller, M. I., Lam, P. J., Moffett, J. W., Till, C. P., Lee, J.-M., Toner, B. M., et al. (2017). Accumulation of Fe oxyhydroxides in the Peruvian oxygen deficient zone implies non-oxygen dependent Fe oxidation. *Geochimica et Cosmochimica Acta* 211, 174–193. doi:10.1016/j.gca.2017.05.019

Ho, T. Y., Quigg, A., Finkel, Z. V., Milligan, A. J., Wyman, K., Falkowski, P. G., et al. (2003). The elemental composition of some marine phytoplankton. *J. Phycol.* 39, 1145–1159. doi:10.1111/j.0022-3646.2003.03-090.x

Hohl, S. V., Galer, S. J. G., Gamper, A., and Becker, H. (2017). Cadmium isotope variations in Neoproterozoic carbonates—a tracer of biologic production? *Geochem. Persp. Lett.* 22, 32–44. doi:10.7185/geochemlet.1704

Hohl, S. V., Jiang, S.-Y., Wei, H.-Z., Pi, D.-H., Liu, Q., Viehmann, S., et al. (2019). Cd isotopes trace periodic (bio)geochemical metal cycling at the verge of the Cambrian animal evolution. *Geochimica et Cosmochimica Acta* 263, 195–214. doi:10.1016/j.gca.2019.07.036

Horner, T. J., Schönbächler, M., Rehkämper, M., Nielsen, S. G., Williams, H., Halliday, A. N., et al. (2010). Ferromanganese crusts as archives of deep water Cd isotope compositions. *Geochem. Geophys. Geosyst.* 11, 121. doi:10.1029/2009gc002987

Horner, T., Lee, R., Henderson, G., and Rickaby, R. E. (2013). Nonspecific uptake and homeostasis drive the oceanic cadmium cycle. *Proc. Natl. Acad. Sci. USA.* 110, 2500–2505. doi:10.1073/pnas.1213857110

Jacobs, L., Emerson, S., and Huested, S. S. (1987). Trace metal geochemistry in the Cariaco trench. *Deep Sea Res. Part A. Oceanogr. Res. Pap.* 34, 965–981. doi:10.1016/0198-0149(87)90048-3

Jacobs, L., Emerson, S., and Skei, J. (1985). Partitioning and transport of metals across the interface in a permanently anoxic basin: framvaren Fjord, Norway. *Geochimica et Cosmochimica Acta* 49, 1433–1444. doi:10.1016/0016-7037(85)90293-5

Jahnke, R. (2010). “Global synthesis”, in *Carbon and nutrient fluxes in continental margins. Global change—the IGBP series*. Editors K. Liu, L. Atkinson, R. Quiñones, and L. Talaue-McManus (Berlin: Springer), 597–615.

Janssen, D., Conway, T., John, S., Christian, J., Kramer, D., Pedersen, T., et al. (2014). Undocumented water column sink for cadmium in open ocean oxygen-deficient zones. *Proc. Natl. Acad. Sci. USA.* 111, 6888–6893. doi:10.1073/pnas.1402388111

Janssen, D. J., Abouchami, W., Galer, S. J. G., and Cullen, J. T. (2017). Fine-scale spatial and interannual cadmium isotope variability in the subarctic northeast Pacific. *Earth and Planetary Science Letters* 472, 241–252. doi:10.1016/j.epsl.2017.04.048

Janssen, D. J., Abouchami, W., Galer, S. J. G., Purdon, K. B., and Cullen, J. T. (2019). Particulate cadmium stable isotopes in the subarctic northeast Pacific reveal dynamic Cd cycling and a new isotopically light Cd sink. *Earth Planet. Sci. Lett.* 515, 67–78. doi:10.1016/j.epsl.2019.03.006

John, S. G., and Conway, T. M. (2014). A role for scavenging in the marine biogeochemical cycling of zinc and zinc isotopes. *Earth Planet. Sci. Lett.* 394, 159–167. doi:10.1016/j.epsl.2014.02.053

John, S. G., Helgoe, J., and Townsend, E. (2018). Biogeochemical cycling of Zn and Cd and their stable isotopes in the eastern tropical south pacific. *Mar. Chem.* 201, 256–262. doi:10.1016/j.marchem.2017.06.001

John, S. G., Kunzmann, M., Townsend, E. J., and Rosenberg, A. D. (2017). Zinc and cadmium stable isotopes in the geological record: a case study from the post-snowball Earth Nuccaleena cap dolostone. *Palaeogeogr. Palaeoclimatol. Palaeoecol.* 466, 202–208. doi:10.1016/j.palaeo.2016.11.003

Jones, M. T., Gislason, S. R., Burton, K. W., Pearce, C. R., Mavromatis, V., Pogge von Strandmann, P. A. E., et al. (2014). Quantifying the impact of riverine particulate dissolution in seawater on ocean chemistry. *Earth Planet. Sci. Lett.* 395, 91–100. doi:10.1016/j.epsl.2014.03.039

Klevenz, V., Bach, W., Schmidt, K., Hentscher, M., Koschinsky, A., and Petersen, S. (2011). Geochemistry of vent fluid particles formed during initial hydrothermal fluid-seawater mixing along the Mid-Atlantic Ridge. *Geochem. Geophys. Geosyst.* 12, 133. doi:10.1029/2011gc003704

Klinkhammer, G., Heggie, D. T., and Graham, D. W. (1982). Metal diagenesis in oxic marine sediments. *Earth Planet. Sci. Lett.* 61, 211–219. doi:10.1016/0012-821X(82)90054-1

Kuss, J., and Kremling, K. (1999). Particulate trace element fluxes in the deep northeast Atlantic Ocean. *Deep Sea Research Part I: Oceanographic Research Papers* 46, 149–169. doi:10.1016/S0967-0637(98)00059-4

Lacan, F., Francois, R., Ji, Y., and Sherrill, R. M. (2006). Cadmium isotopic composition in the ocean. *Geochimica et Cosmochimica Acta* 70, 5104–5118. doi:10.1016/j.gca.2006.07.036

Lambelet, M., Rehkämper, M., van de Flierdt, T., Xue, Z., Kreissig, K., Coles, B., et al. (2013). Isotopic analysis of Cd in the mixing zone of Siberian rivers with the Arctic Ocean—New constraints on marine Cd cycling and the isotope composition of riverine Cd. *Earth Planet. Sci. Lett.* 361, 64–73. doi:10.1016/j.epsl.2012.11.034

Lane, T., Saito, M., George, G., Pickering, I., Prince, R., and Morel, F. M. (2005). A cadmium enzyme from a marine diatom. *Nature* 435, 42. doi:10.1038/435042a

Lee, J.-M., Heller, M. I., and Lam, P. J. (2018). Size distribution of particulate trace elements in the U.S. GEOTRACES eastern pacific zonal transect (GP16). *Mar. Chem.* 201, 108–123. doi:10.1016/j.marchem.2017.09.006

Little, S. H., Vance, D., Lyons, T. W., and McManus, J. (2015). Controls on trace metal authigenic enrichment in reducing sediments: insights from modern oxygen-deficient settings. *Am. J. Sci.* 315, 77–119. doi:10.2475/02.2015.01

Little, S. H., Vance, D., McManus, J., and Severmann, S. (2016). Key role of continental margin sediments in the oceanic mass balance of Zn and Zn isotopes. *Geology* 44, 207–210. doi:10.1130/g37493.1

Little, S. H., Vance, D., McManus, J., Severmann, S., and Lyons, T. W. (2017). Copper isotope signatures in modern marine sediments. *Geochimica et Cosmochimica Acta* 212, 253–273. doi:10.1016/j.gca.2017.06.019

Marchitto, T. M., and Broecker, W. S. (2006). Deep water mass geometry in the glacial Atlantic Ocean: a review of constraints from the paleonutrient proxy Cd/Ca. *Geochem. Geophys. Geosyst.* 7, a. doi:10.1029/2006gc001323

Martin, J. H., Bruland, K. W., and Broenkow, W. W. (1976). “Cadmium transport in the California current,” in . Editors H. L. Windom and R. A. Duce (Lexington, MA: D. C. Heath), 159–184.

Martin, J. H., and Knauer, G. A. (1973). The elemental composition of plankton. *Geochimica et Cosmochimica Acta* 37, 1639–1653. doi:10.1016/0016-7037(73)90154-3

McCorkle, D. C., and Klinkhammer, G. P. (1991). Porewater cadmium geochemistry and the porewater cadmium:δ¹³C relationship. *Geochimica et Cosmochimica Acta* 55, 161–168. doi:10.1016/0016-7037(91)90408-w

McManus, J., Berelson, W. M., Coale, K. H., Johnson, K. S., and Kilgore, T. E. (1997). Phosphorus regeneration in continental margin sediments. *Geochimica et Cosmochimica Acta* 61, 2891–2907. doi:10.1016/s0016-7037(97)00138-5

McManus, J., Berelson, W. M., Klinkhammer, G. P., Johnson, K. S., Coale, K. H., Anderson, R. F., et al. (1998). Geochemistry of barium in marine sediments: implications for its use as a paleoproxy. *Geochimica et Cosmochimica Acta* 62, 3453–3473. doi:10.1016/s0016-7037(98)00248-8

McManus, J., Berelson, W. M., Klinkhammer, G. P., Johnson, K. S., Coale, K. H., Anderson, R. F., et al. (2006). Molybdenum and uranium geochemistry in continental margin sediments: paleoproxy potential. *Geochimica et Cosmochimica Acta* 70, 4643–4662. doi:10.1016/j.gca.2006.06.1564

Middag, R., van Heuven, S. M. A. C., Bruland, K. W., and de Baar, H. J. W. (2018). The relationship between cadmium and phosphate in the Atlantic Ocean unravelled. *Earth Planet. Sci. Lett.* 492, 79–88. doi:10.1016/j.epsl.2018.03.046

Moore, C. M., Mills, M. M., Arrigo, K. R., Berman-Frank, I., Bopp, L., and Boyd, P. W. (2013). Processes and patterns of oceanic nutrient limitation. *Nature Geosci.* 6, 701–710. doi:10.1038/ngeo1765

Morfod, J. L., and Emerson, S. (1999). The geochemistry of redox sensitive trace metals in sediments. *Geochimica et Cosmochimica Acta* 63, 1735–1750. doi:10.1016/s0016-7037(99)00126-x

Morse, J. W., and Luther, G. W., III (1999). Chemical influences on trace metal-sulfide interactions in anoxic sediments. *Geochimica et Cosmochimica Acta* 63, 3373–3378. doi:10.1016/S0016-7037(99)00258-6

Murphy, K., Rehkämper, M., Kreissig, K., Coles, B., and van de Flierdt, T. (2016). Improvements in Cd stable isotope analysis achieved through use of liquid-liquid extraction to remove organic residues from Cd separates obtained by extraction chromatography. *J. Anal. Spectrom.* 31, 319–327. doi:10.1039/c5ja00115c

Nriagu, J. O. (1980). “Cadmium in the atmosphere and in precipitation,” Part 1 in *Cadmium in the environment. Ecological cycling*. Editor Nriagu, J. O. (New York, NY: John Wiley), 71–114.

Ohnemus, D. C., Rauschenberg, S., Cutter, G. A., Fitzsimmons, J. N., Sherrill, R. M., and Twining, B. S. (2016). Elevated trace metal content of prokaryotic communities associated with marine oxygen deficient zones. *Limnol. Oceanogr.* 62, 3–25. doi:10.1002/lo.10363

Patterson, T. L., and Duce, R. A. (1991). The cycle of atmospheric cadmium over the North Pacific Ocean. *Tellus B: Chem. Phys. Meteorol.* 43, 12–29. doi:10.3402/tellusb.v43i1.15243

Plass, A., Schlosser, C., Sommer, S., Dale, A. W., Achterberg, E. P., and Scholz, F. (2020). The control of hydrogen sulfide on benthic iron and cadmium fluxes in the oxygen minimum zone off Peru. *Biogeosciences* 17, 3685–3704. doi:10.5194/bg-2019-39010.5194/bg-17-3685-2020

Poulson Brucker, R. L., McManus, J., Severmann, S., and Berelson, W. M. (2009). Molybdenum behavior during early diagenesis: insights from Mo isotopes. *Geochim. Geophys. Geosyst.* 10, a. doi:10.1029/2008gc002180

Price, N. M., and Morel, F. M. M. (1990). Cadmium and cobalt substitution for zinc in a marine diatom. *Nature* 344, 658–660. doi:10.1038/344658a0

Quay, P., Cullen, J., Landing, W., and Morton, P. (2015). Processes controlling the distributions of Cd and PO4 in the ocean. *Glob. Biogeochem. Cycles* 29, 830–841. doi:10.1002/2014gb004998

Ripperger, S., Rehkämper, M., Porcelli, D., and Halliday, A. N. (2007). Cadmium isotope fractionation in seawater—a signature of biological activity. *Earth Planet. Sci. Lett.* 261, 670–684. doi:10.1016/j.epsl.2007.07.034

Ripperger, S., and Rehkämper, M. (2007). Precise determination of cadmium isotope fractionation in seawater by double spike MC-ICPMS. *Geochimica et Cosmochimica Acta* 71, 631–642. doi:10.1016/j.gca.2006.10.005

Rosenthal, Y., Lam, P., Boyle, E. A., and Thomson, J. (1995). Authigenic cadmium enrichments in suboxic sediments: precipitation and postdepositional mobility. *Earth Planet. Sci. Lett.* 132, 99–111. doi:10.1016/0012-821x(95)00056-i

Rudnick, R. L., and Gao, S. (2003). *Composition of the continental crust* 3. Oxford: Elsevier-Pergamon, 1–64. doi:10.1016/b0-08-043751-6/03016-4

Schlitzer, R. (2017). Ocean data view. odv.awi.de.

Schmitt, A.-D., Galer, S. J. G., and Abouchami, W. (2009). Mass-dependent cadmium isotopic variations in nature with emphasis on the marine environment. *Earth Planet. Sci. Lett.* 277, 262–272. doi:10.1016/j.epsl.2008.10.025

Scholz, F., Löscher, C. R., Fiskal, A., Sommer, S., Hensen, C., Lomnitz, U., et al. (2016). Nitrate-dependent iron oxidation limits iron transport in anoxic ocean regions. *Earth Planet. Sci. Lett.* 454, 272–281. doi:10.1016/j.epsl.2016.09.025

Scholz, F., Severmann, S., McManus, J., and Hensen, C. (2014). Beyond the Black Sea paradigm: the sedimentary fingerprint of an open-marine iron shuttle. *Geochimica et Cosmochimica Acta* 127, 368–380. doi:10.1016/j.gca.2013.11.041

Schunck, H., Lavik, G., Desai, D., Großkopf, T., Kalvelage, T., Löscher, C., et al. (2013). Giant hydrogen sulfide plume in the oxygen minimum zone off Peru supports chemolithoautotrophy. *PLoS ONE* 8, e68661. doi:10.1371/journal.pone.0068661

Severmann, S., Johnson, C. M., Beard, B. L., and McManus, J. (2006). The effect of early diagenesis on the Fe isotope compositions of porewaters and authigenic minerals in continental margin sediments. *Geochimica et Cosmochimica Acta* 70, 2006–2022. doi:10.1016/j.gca.2006.01.007

Severmann, S., McManus, J., Berelson, W. M., and Hammond, D. E. (2010). The continental shelf benthic iron flux and its isotope composition. *Geochimica et Cosmochimica Acta* 74, 3984–4004. doi:10.1016/j.gca.2010.04.022

Shaw, T. J., Gieskes, J. M., and Jahnke, R. A. (1990). Early diagenesis in differing depositional environments: the response of transition metals in pore water. *Geochimica et Cosmochimica Acta* 54, 1233–1246. doi:10.1016/0016-7037(90)90149-f

Sieber, M., Conway, T. M., de Souza, G. F., Hassler, C. S., Ellwood, M. J., and Vance, D. (2019a). High-resolution Cd isotope systematics in multiple zones of the southern ocean from the antarctic circumnavigation expedition. *Earth Planet. Sci. Lett.* 527, 115799. doi:10.1016/j.epsl.2019.115799

Sieber, M., Conway, T. M., de Souza, G. F., Obata, H., Takano, S., Sohrin, Y., et al. (2019b). Physical and biogeochemical controls on the distribution of dissolved cadmium and its isotopes in the Southwest Pacific Ocean. *Chem. Geology.* 511, 494–509. doi:10.1016/j.chemgeo.2018.07.021

Siebert, C., Nägler, T. F., and Kramers, J. D. (2001). Determination of molybdenum isotope fractionation by double-spike multicollector inductively coupled plasma mass spectrometry. *Geochim. Geophys. Geosyst.* 2, 39. doi:10.1029/2000gc000124

Silverberg, N., Martinez, A., Aguiñiga, S., Carriquiry, J. D., Romero, N., Shumilin, E., et al. (2004). Contrasts in sedimentation flux below the southern California Current in late 1996 and during the El Niño event of 1997–1998. *Estuarine, Coastal Shelf Sci.* 59, 575–587. doi:10.1016/j.ecss.2003.11.003

Sunda, W. G., and Huntsman, S. A. (1998). Control of Cd concentrations in a coastal diatom by interactions among free ionic Cd, Zn, and Mn in seawater. *Environ. Sci. Technol.* 32, 2961–2968. doi:10.1021/es980271y

Sunda, W. G., and Huntsman, S. A. (2000). Effect of Zn, Mn, and Fe on Cd accumulation in phytoplankton: implications for oceanic Cd cycling. *Limnol. Oceanogr.* 45, 1501–1516. doi:10.4319/lo.2000.45.7.1501

Sweere, T. C., Dickson, A. J., Jenkyns, H. C., Porcelli, D., Ruhl, M., Murphy, M. J., et al. (2020). Controls on the Cd-isotope composition of upper cretaceous (Cenomanian–Turonian) organic-rich mudrocks from south Texas (eagle ford group). *Geochimica et Cosmochimica Acta* 287, 251. doi:10.1016/j.gca.2020.02.019

Tankré, S. P. C., Muller, F. L. L., Burton, J. D., Statham, P. J., Guieu, C., and Martin, J.-M. (2001). Trace metal distributions in shelf waters of the northwestern Black Sea. *Continental Shelf Res.* 21, 1501–1532. doi:10.1016/s0278-4343(01)00013-9

Thunell, R. C., Tappa, E., and Anderson, D. M. (1995). Sediment fluxes and varve formation in Santa Barbara Basin, offshore California. *Geology* 23, 1083. doi:10.1130/0091-7613(1995)023<1083:sfavfi>2.3.co;2

van Geen, A., McCorkle, D. C., and Klinkhammer, G. P. (1995). Sensitivity of the phosphate-cadmium-carbon isotope relation in the ocean to cadmium removal by suboxic sediments. *Paleoceanography* 10, 159–169. doi:10.1029/94pa03352

van Geen, A., Zheng, Y., Bernhard, J. M., Cannariato, K. G., Carriquiry, J., Dean, W. E., et al. (2003). On the preservation of laminated sediments along the western margin of North America. *Paleoceanography* 18, 121. doi:10.1029/2003PA000911

Von Damm, K. L., Edmond, J. M., Grant, B., Measures, C. I., Walden, B., and Weiss, R. F. (1985). Chemistry of submarine hydrothermal solutions at 21° N, East Pacific Rise. *Geochimica et Cosmochimica Acta* 49, 2197–2220. doi:10.1016/0016-7037(85)90222-4

Waelies, M., Riso, R. D., and Le Corre, P. (2005). Seasonal variations of cadmium speciation in the Penzé estuary, NW France. *Estuarine, Coastal Shelf Sci.* 65, 143–152. doi:10.1016/j.ecss.2005.06.002

Waelies, M., Riso, R. D., Maguer, J.-F., and Le Corre, P. (2004). Distribution and chemical speciation of dissolved cadmium and copper in the Loire estuary and North Biscay continental shelf, France. *Estuarine, Coastal Shelf Sci.* 59, 49–57. doi:10.1016/j.ecss.2003.07.009

Waldron, K., and Robinson, N. J. (2009). How do bacterial cells ensure that metalloproteins get the correct metal?. *Nat. Rev. Microbiol.* 7, 25–35. doi:10.1038/nrmicro2057

Wasylewski, L. E., Swihart, J. W., and Romaniello, S. J. (2014). Cadmium isotope fractionation during adsorption to Mn oxyhydroxide at low and high ionic strength. *Geochimica et Cosmochimica Acta* 140, 212–226. doi:10.1016/j.gca.2014.05.007

Westerlund, S. F. G., Anderson, L. G., Hall, P. O. J., Iverfeldt, Å., Van Der Loeff, M. M. R., and Sundby, B. (1986). Benthic fluxes of cadmium, copper, nickel, zinc and lead in the coastal environment. *Geochimica et Cosmochimica Acta* 50, 1289–1296. doi:10.1016/0016-7037(86)90412-6

Xie, R. C., Galer, S. J. G., Abouchami, W., and Frank, M. (2019a). Limited impact of eolian and riverine sources on the biogeochemical cycling of Cd in the tropical Atlantic. *Chem. Geol.* 511, 371–379. doi:10.1016/j.chemgeo.2018.10.018

Xie, R. C., Galer, S. J. G., Abouchami, W., Rijkenberg, M. J. A., de Baar, H. J. W., De Jong, J., et al. (2017). Non-Rayleigh control of upper-ocean Cd isotope fractionation in the western South Atlantic. *Earth Planet. Sci. Lett.* 471, 94–103. doi:10.1016/j.epsl.2017.04.024

Xie, R. C., Rehkämper, M., Grasse, P., van de Flierdt, T., Frank, M., and Xue, Z. (2019b). Isotopic evidence for complex biogeochemical cycling of Cd in the eastern tropical South Pacific. *Earth Planet. Sci. Lett.* 512, 134–146. doi:10.1016/j.epsl.2019.02.001

Xu, Y., Feng, L., Jeffrey, P., Shi, Y., and Morel, F. M. (2008). Structure and metal exchange in the cadmium carbonic anhydrase of marine diatoms. *Nature* 452, 56–61. doi:10.1038/nature06636

Xu, Y., Tang, D., Shaked, Y., and Morel, F. M. M. (2007). Zinc, cadmium, and cobalt interreplacement and relative use efficiencies in the coccolithophore *Emiliania huxleyi*. *Limnol. Oceanogr.* 52, 2294–2305. doi:10.4319/lo.2007.52.5.2294

Xue, Z., Rehkämper, M., Schönbachler, M., Statham, P., and Coles, B. J. (2012). A new methodology for precise cadmium isotope analyses of seawater. *Anal. Bioanal. Chem.* 402, 883–893. doi:10.1007/s00216-011-5487-0

Xue, Z., Rehkämper, M., Horner, T. J., Abouchami, W., Middag, R., van de Flierd, T., et al. (2013). Cadmium isotope variations in the southern ocean. *Earth Planet. Sci. Lett.* 382, 161–172. doi:10.1016/j.epsl.2013.09.014

Yang, S.-C., Lee, D.-C., and Ho, T.-Y. (2015). Cd isotopic composition in the suspended and sinking particles of the surface water of the South China Sea: the effects of biotic activities. *Earth Planet. Sci. Lett.* 428, 63–72. doi:10.1016/j.epsl.2015.07.025

Yang, S.-C., Zhang, J., Sohrin, Y., and Ho, T.-Y. (2018). Cadmium cycling in the water column of the Kuroshio-Oyashio Extension region: insights from dissolved and particulate isotopic composition. *Geochimica et Cosmochimica Acta* 233, 66–80. doi:10.1016/j.gca.2018.05.001

Conflict of Interest: The authors declare that the research was conducted in the absence of any commercial or financial relationships that could be construed as a potential conflict of interest.

Copyright © 2021 Chen, Little, Kreissig, Severmann and McManus. This is an open-access article distributed under the terms of the Creative Commons Attribution License (CC BY). The use, distribution or reproduction in other forums is permitted, provided the original author(s) and the copyright owner(s) are credited and that the original publication in this journal is cited, in accordance with accepted academic practice. No use, distribution or reproduction is permitted which does not comply with these terms.